IN SEARCH OF THE PROXIMATE FACTORS TRIGGERING ANTHRAX EPIDEMICS: SIMULATION OF PLASMID TRANSFER AND PERSISTENCE IN *BACILLUS* COMMUNITIES OUTSIDE OF THE HOST

An Undergraduate Research Scholars Thesis

by

ALEXANDRA E. BISHOP

Submitted to the Undergraduate Research Scholars program at
Texas A&M University
in partial fulfillment of the requirements for the designation as an

UNDERGRADUATE RESEARCH SCHOLAR

Approved by Research Advisor: Dr. Hsiao-Hsuan Wang

May 2020

Major: Biology

TABLE OF CONTENTS

ABSTRACT

In Search of the Proximate Factors Triggering Anthrax Epidemics: Simulation of Plasmid Transfer and Persistence in *Bacillus* Communities Outside of the Host

Alexandra E. Bishop
Department of Biology
Texas A&M University

Research Advisor: Dr. Hsiao-Hsuan Wang
Department of Wildlife and Fisheries Sciences
Texas A&M University

A bacterial infection popularized through bioterrorism, anthrax is a potentially fatal illness. *Bacillus anthracis*, notoriously the causative agent of anthrax, exists in community with hundreds of other species of bacteria in the environment, and is known to harbor in the rhizosphere of grass roots. Recent work done on the genetics of these communities has shown that *B. anthracis* shares a very high percentage of chromosomal genes with both *B. thuringiensis* and *B. cereus*, and that phenotypic differences between the bacterium results from extra-chromosomal DNA, usually plasmids. Therefore, the ability of *B. anthracis* to produce anthrax toxins is transmittable to other bacterium within its community, under the correct conditions. Following a literature review, I aimed to develop a model of bacterial conjugation within the *Bacillus* genus. I developed a spatially-explicit, individual-based, stochastic simulation model using NetLogo, an agent-based modeling language, for investigating the likelihood of detecting plasmids with genes encoding anthrax toxins within bacterial communities composed of *B. anthracis*, *B. thuringiensis*, *B. cereus*, and the surrounding matrix of extra-cellular polymeric substances. Model evaluation results indicate that the model shows promise as a simple, useful

representation of the pertinent characteristics of the system of interest, and confirm the potential of the horizontal transfer of plasmids with genes encoding anthrax toxins among *Bacillus* species persisting outside the host as a proximate factor triggering anthrax epidemics. Further model demonstration has showed that the predictions and data produced by the model are compatible with data in the literature.

ACKNOWLEDGMENTS

The completion of this dissertation could not have been possible without constant and thoughtful guidance from my research advisor Dr. Hsiao-Hsuan Wang. For this I am deeply indebted and sincerely thankful. Her invaluable guidance throughout this entire process has been invaluable in my development as a young scientist.

I would also like to thank my family for their never-ending support of my education, and their encouragement to get involved in research. Without them, this would not have been possible.

CHAPTER I

INTRODUCTION

From a human perspective, a common characteristic of many disease-causing agents is their ability to appear and disappear quickly in nature, often in an inexplicable manner (Salkeld et al., 2010). The bacterium *Bacillus anthracis* is notorious among the general public as the causative agent of anthrax and as a potential weapon of bioterrorists (Schwartz, 2009). It is equally notorious among scientists and disease control specialists for its ability to disappear suddenly, even after major outbreaks (Kiel et al., 2009).

At the macro level, anthrax spores have been found throughout the world (Goel, 2015), and quantitative models describing the documented (Blackburn et al., 2017), and projecting the potential (Barro et. al., 2016) geographic distribution of anthrax abound. Many studies have correlated reported cases of anthrax with physical environmental factors (Blackburn, 2006) and with the distribution of potential vectors (Blackburn, 2006). However, while macro-scale correlative models are useful in delineating areas of high risk where anthrax or its components are or were present, they are less useful in providing information that could be used to design preemptive management schemes on finer spatial and temporal scales. The latter requires an understanding of the conditions fostering appearance of the pathogen in a form capable of producing an epidemic (Kiel et al., 2009).

At the micro level, *Bacillus* and other bacteria exist in communities composed of potentially hundreds of species. The complexity and plasticity of ecological and evolutionary relationships within microbial communities is well documented (Czárán and Hoekstra, 2009; Faust et. al., 2012). Bacterial plasmids (extra-chromosomal genetic elements that code for a wide

variety of phenotypes in their bacterial hosts and which are maintained in bacterial communities through both vertical and horizonal transfer) contribute significantly to this plasticity and complexity (Saile and Koehler, 2006; Pena-Gonzalez 2018).

Recent work on the genetics of *B. anthracis* and other *Bacillus* species has suggested that *B. anthracis*, *B. thuringiensis* (an important source of insecticidal toxins), and *B. cereus* (a ubiquitous soil bacterium and opportunistic human pathogen) have a very high degree of genetic similarity based on their chromosomal genes (slightly below ≈92.5 ANI), with extra-chromosomal DNA, usually present as plasmids, accounting for many phenotypic differences (Helgason et al., 2000; Carroll et al., 2019). In fact, there are known cases of a human diagnosed with inhalation anthrax that revealed infection with bacteria identified as *B. cereus*, not *B. anthracis*. However, further examination identified the presence of the two plasmids with genes encoding anthrax toxins within the *B. cereus* cells (Hoffmaster et al., 2004). In *B. anthracis*, the anthrax toxin and capsule genes responsible for anthrax disease are located on the pXo1 and pXo2 plasmids, respectively (Okinaka et al., 1999; Taylor-Joyce et al., 2019). These plasmids are not self-transmissible but can be mobilized by conjugative plasmids, such as pXo14 or pXo16 from *B. thuringiensis* (Reddy et al., 1987; Hinnekens et al., 2019). Hu et al. (2009) recently have documented the distribution, diversity, and potential mobility of extrachromosomal elements related to the *B. anthracis* pXo1 and pXo2 plasmids.

The fact that species related to *B. anthracis, B. thuringiensis,* and *B. cereus* can share bacteriophages, plasmids, and other genetic material suggests that they must grow in environmental niches that provide the opportunity for such exchange. Although relatively little is known about the ecology of *B. anthracis* outside of the host, past studies have documented that it can survive as a saprophyte in the soil and can establish vegetative cells that support horizontal

gene transfer in the rhizosphere of grass plants (Saile and Koehler, 2006). These results suggest that horizontal plasmid transfer among *Bacillus* species persisting outside the host may provide important clues in the search for the proximate factors triggering anthrax epidemics, and that the causative agent may not be *B. anthracis* per se. More specifically, we hypothesize that the biodiversity of bacterial communities may be linked to anthrax outbreaks in a manner analogous to the manner in which prevalence of vector-borne infectious diseases has been linked to biodiversity of their host communities (Keesing et al., 2010).

Vector-borne pathogens often have multiple hosts whose densities vary widely in time and space, and who have very different transmission capabilities, thus providing two mechanisms for diluting or intensifying the rate of disease spread. Sudden outbreaks of plague in prairie dog populations in North American grasslands have been linked to population fluctuations coupled with spatially-restricted movement patterns of grasshopper mice, which carry fleas with plague (Salkeld et al., 2010). When grasshopper mice populations are low, movement of fleas amount prairie dog colonies is restricted and plague remains enzootic; when populations are high, grasshopper mice provide a flea/plague transmission network connecting colonies and triggering an outbreak. Similarly, prevalence of Lyme disease in the northeastern United States has been linked to host community composition (LoGiudice et al., 2003; Granter et al., 2014). Disease prevalence is higher in areas of reduced biodiversity dominated by white-footed mice, which have a high competence to transmit the Lyme pathogen, and lower in areas of higher host diversity in which the majority of hosts have a low transmission competence.

In the case of anthrax, the same two mechanisms may be operating in a similar manner, albeit on different spatial and temporal scales. Concentrations of plasmid-bearing genes encoding anthrax toxins may be diluted or intensified by spatial and temporal variation in the composition

of bacterial communities, since different species have markedly different segregation loss rates. A study by Krone et al. (2007) of plasmid transfer in bacterial micro-colonies and biofilms has identified the importance of spatial structure in determining the rates of plasmid transfer and persistence in such communities, while another recent article has documented drastic differences in bacterial biodiversity in the ecosystem inside a pitcher plant due solely to the presence or absence of a mosquito larvae (Kolter, 2010). The same article (Kolter, 2010) documented a correlation between human lung function and bacterial community diversity in the respiratory tract. Subjects with healthy lungs had diverse communities, whereas patients suffering from cystic fibrosis had less diverse communities dominated by *Pseudomonas aeruginosa* (the predominant pathogen of cystic fibrosis).

Recent studies have found a high abundance and diversity of *B. anthracis* pXo1-like plasmid replicons (*repX*) in various environmental settings not known to contain *B. anthracis* (Bahl and Rosenberg, 2010; Akhtar and Khan, 2012). Furthermore, some of the same *B. cereus* group strains that contained *repX* gene sequences with high homology to the *repX* gene of plasmid pXo1 also contained replicon-specific sequences with high homology to those of pXo2-like plasmids, although they did not contain the pXo1-associated *cya* and *lef* virulence genes. The presence of both pXo1-like and pXo2-like plasmids in the same environmental settings suggests the backbone genes of these plasmids may be abundant in various environmental settings not suspected of containing *B. anthracis* and may co-reside in the same host strains (Bahl and Rosenberg, 2010). This suggests the species classification with the *B. cereus* group may not be particularly useful in describing their virulence profile and in predicting their potential to trigger anthrax epidemics.

There has been much experimental and theoretical work focused on the processes and factors that govern plasmid transfer via bacterial conjugation. Conjugation rates change in relation to biotic and abiotic factors which include cell metabolic activity, bacterial cell diversity, plasmid donor and recipient relatedness, nutrient availability and the spatial architecture of the bacterial community (Seoane et al., 2010a). Studies of plasmid invasion of bacterial communities are providing new insights into both the evolution of microorganisms and the potential benefits and risks of human manipulation of such invasions (Birge, 2013; Maloy et al., 1994).

Recent studies have documented the importance of extra-cellular chemical signaling in controlling the dynamics of bacterial communities (Czárán and Hoekstra, 2009) and in biofilm formation (Sharma et al., 2019), as well as the potential role of such chemical signals in linking biofilms with their external environment (Wood et al., 2010). Current studies are investigating the possibility of manipulating the structure and function of bacterial communities via the introduction of specific signaling chemicals (Wood et al., 2010). Thus, it seems plausible to suggest the possibility of linking anthrax outbreaks to the horizontal transfer within bacterial communities of plasmids carrying the genes encoding the anthrax toxin, and to potentially control transfer rates via externally supplied chemical signals. A bacteriolytic agent capable of detecting and killing *B. anthracis* and other members of the *B. anthracis* "cluster" of bacilli has been identified (Schuch et al., 2002). However, less intrusive and longer-acting chemical signals would be desirable.

For the investigation of plasmid invasion and extra-cellular chemical signaling in bacterial communities, where dimensionality in space and time are important factors, an individual-based approach seems more appropriate both computationally (Sonenshine and Mather, 1994; Gregory et al., 2010) and experimentally (Seoane et al., 2010a). The most relevant

parameters describing a conjugation event at the individual cell level in a structured environment are: (1) the conjugation rate, (2) the donor-recipient distance, and (3) the lag times between plasmid receipt and plasmid transfer (Seoane 2010b). Although the majority of parameter estimates currently available are based on population-level averages, the rapid development of individual-based observational technology (Brehm-Stecher and Johnson, 2004) has provided the opportunity for experiments yielding estimates of plasmid transfer efficiencies at the individual cell scale (Seoane et al., 2010a).

As a proof of concept, I have developed a relatively simple, individual-based model to simulate the potential spread of pXo1 and pXo2 plasmids within bacterial communities composed of *B. anthracis*, *B. thuringiensis*, *B. cereus*, and the surrounding matrix of extra-cellular polymeric substances. A variety of much more sophisticated models bacteria are available, which, depending on the particular questions addressed, have included detailed mechanistic representations of metabolic pathways and genetic control networks, e.g., Abedon et al. (2001), Evans et al. (2007), Laschov and Margaliot (2009), and Payne and Jansen (2001), or sophisticated sets of rules for individual-based models, e.g., Gregory et al. (2008) and Vlachos et al. (2006). The challenge is to design a model based on processes simple enough to be understood that also can generate simulated patterns that can be tested experimentally (Grimm and Railsback, 2005).

In this paper, I present a spatially-structured, individual-based, stochastic simulation model developed to investigate the likelihood of detecting plasmids with genes encoding anthrax toxins within bacterial communities composed of *B. anthracis*, *B. thuringiensis*, *B. cereus*, and the surrounding matrix of extra-cellular polymeric substances. In the sections that follow, I first describe the model, following the protocol suggested for individual-/agent-based models by

Grimm et al. (2006). I then evaluate model performance by verifying that simulated patterns of bacterial processes agree with those reported in literature upon which I had based model parameterization, and by assessing the ability of the model to simulate bacterial root surface colonization and dynamics. Next, I evaluate model performance under field conditions by examining the sensitivity of simulated bacterial community dynamics to changes in climatic conditions and initial bacterial community composition. Finally, I will demonstrate application of the model by simulating bacterial community dynamics on the surface of a hypothetical plant root, establishing a baseline for initial species densities, and running an experimental simulation in assuming that *B. thuringiensis* cannot conjugate while recording the temporal dynamics of each species of bacteria.

CHAPTER II

MODEL DESCRIPTION

A) Purpose

The purpose of the model was to stimulate the spatial-temporal dynamics of bacterial communities (composed of *B. anthracis, B. thuringiensis, B. cereus*, and the surrounding matrix of extra-cellular polymeric substances) on the surface of a hypothetical plant root in order to investigate the likelihood of detecting plasmids with genes encoding anthrax toxins (Appendix II Figure 1).

B) State Variables and Scales

State variables included (1) 2,500, 20.5 μm x 20.5 μm (2 μm^2) habitat cells arrayed in a 50 x 50 habitat grid (total area = 5 mm^2), (2) up to 5,000 bacteria (maximum 2 per habitat cell), and (3) up to several thousand plasmids (Appendix I Table 1a). Attributes of habitat cells included identification number, location, whether or not they contained a plant root, nutrient level, and rate of nutrient renewal. Attributes of bacteria included identification number, species, state (active or spore), nutrient requirement, nutrients accumulated since last cell division, starvation level (number of consecutive 5-minute time steps without consuming nutrients), and identification numbers of the Xo1, Xo2, and Xo16 plasmids within the bacterial cell. Attributes of plasmids included identification number, kind (Xo1, Xo2, and Xo16), identification number of the bacterium in which they are located (or "-1" if extra-cellular), state (active or in spore), and number of conjugation events. System-level auxiliary variables included total number of active and inactive bacterial cells and numbers of active and inactive *B. anthracis, B. thuringiensis, B. cereus*, as well as the numbers of the Xo1, Xo2, and Xo16 plasmids in active bacteria, in spores,

and in the extra-cellular matrix (Appendix II Table 1b). Auxiliary variables and attributes of state variables that could change over time were updated at 5-minute intervals.

I based the determination of spatial and temporal scales on the ecology of the organisms involved, the level of detail contained in available information, and computational considerations. This spatial scale allowed adequate representation of the (implicit) positioning of bacterial cells for conjugation (I assumed an average cell size of 1 μm2 and, thus, a maximum of two bacterial cells per habitat cell) (Krone et al., 2007), as well as adequate representation of the spread of plasmids through the bacterial colony (Seoane et al., 2010). This temporal scale provided adequate resolution to represent the effects of temperature (Zwietering et al., 1991) and relative humidity (Iturriaga et al., 2007) on bacterial growth rates and associated processes (processes occur at rates scaled to baseline rates that represent a system in which the doubling time of *Bacillus* species would be ≈ 40 minutes at 30C and 100% relative humidity when nutrients are not limited).

C) Process Overview and Scheduling

I programmed the model and executed simulations in NetLogo ((http://ccl.northwestern.edu/netlogo/). During each simulation, the system is initialized by describing the numbers, types, and spatial distribution of bacteria and plasmids, and the amount and spatial distribution of nutrients (Appendix II Figure 2). Next, iteratively, for each 5-minute time step, (1) climatic conditions are updated and associated potential bacterial growth rates are calculated, (2) plant root growth occurs and nutrient levels in each habitat cell are updated, and (3) plasmid degradation, (4) spore formation, (5) nutrient consumption, (6) bacterial death occur, (7) reproduction and segregative loss, (8) conjugation, (11) transformation, and (12) germination occur. I discuss the conceptual design details for process scheduling in Section D.

D) Design Concepts

D1) Emergence

Spatial and temporal patterns of nutrients emerge as system-level properties as a result of rates of nutrient renewal of individual habitat cells, which depends on the presence or absence of plant roots, and rates of nutrient consumption by individual bacteria. Spatial and temporal patterns of vegetative (active) cells and spores of *B. anthracis, B. thuringiensis, and B. cereus* emerge as a result of the reproduction, death, spore formation, and germination of individual bacteria. Spatial and temporal patterns of Xo1, Xo2, and Xo16 plasmids, both within bacteria and in the surrounding matrix of extra-cellular polymeric substances, emerge as a result of the reproduction, segregative loss, conjugation, transformation, and death of individual bacteria, as well as via the degradation of individual plasmids.

D2) Sensing

Individual bacteria, in addition to being aware of their own species and state, which affect all of their behavior, also are aware of (1) the nutrient level in each habitat cell within their "nutrient neighborhood" (described in Section G5), which affects their rate of consumption, (2) the number of bacteria of each species in each habitat cell within their "growth neighborhood" (described in Section G7), which affects their rates of reproduction and conjugation, (3) the number of plasmids of each kind within each bacterium (including themselves) within their growth neighborhood, which affects their rates of conjugation, (4) the number of extra-cellular plasmids of each kind in each habitat cell within their growth neighborhood, which affects their rate of transformation, and (6) their own starvation level, which affects their rates of spore formation and death. Individual plasmids are aware of their own kind, state, and number of previous conjugation events, and whether or not they are currently in a bacterium, which affects

their rates of horizontal transfer during bacterial conjugation, their rates of extra-cellular degradation, and their rates of "pickup" from the extra-cellular matrix during bacterial transformation.

D3) Interaction

Interactions occur between individual bacteria explicitly during conjugation via the exchange of plasmids, and implicitly during reproduction via the suppression of cell division if the growth neighborhood is fully occupied. Interactions occur implicitly between individual bacteria and individual plasmids during conjugation and transformation via the suppression of these processes depending on the plasmids already within the potentially conjugating or transforming bacteria, and during the death of bacteria via the release of plasmids into the extra-cellular matrix. Interactions also occur implicitly between individual plasmids during conjugation and transformation via the suppression of these processes.

D4) Stochasticity

Individual bacteria are activated, and plasmids are assigned to bacteria and to the extra-cellular matrix of habitat cells randomly at the beginning of simulations, depending on the scenario being simulated. All processes in the model are calculated probabilistically. The importance of capturing the stochastic nature of the spread of microbial communities in spatially structured habitats is well recognized (Kreft et al., 1998; Wei and Krone, 2005; Krone et al., 2007).

D5) Scheduling Details

To initiate each 5-minute time step, first climatic conditions are updated and associated potential bacterial growth rates are calculated (Appendix II Figure 2). Then, plant root growth occurs and habitat nutrient levels are updated. Plasmid degradation then occurs. These processes

do not involve interaction among system components. Next, the bacterial processes of spore formation, nutrient consumption, death, reproduction and segregative loss, conjugation, transformation, and germination occur sequentially. Each bacterium, in random order, is given the opportunity to perform each process before the model proceeds to the next process, with the system updated after each action. Since these processes involve either direct or indirect "simultaneous" interaction among all system components, the bias created by sequential processing is minimized by randomizing the order in which individual bacteria perform their activities. Since individual plasmids do not initiate any actions, except their own degradation in the extra-cellular matrix, randomization of the order in which individual bacteria act also minimizes the effect of sequential processing on individual plasmids.

D6) Observation

During model evaluation, that is, to evaluate the capability of the model to generate reasonable patterns of bacterial growth, conjugation, and transformation, I monitored the spatial-temporal dynamics of bacteria and plasmids from an omniscient perspective. During model application, to investigate the likelihood of detecting plasmids with genes encoding anthrax toxins on the surface of a hypothetical plant root, I sampled conjugation, segregative loss, and transformation levels in response to different environmental factors from the perspective of a virtual ecologist.

E) Initialization

The system is initialized by describing the numbers, types, and spatial distributions of bacteria, plasmids, and the amount and spatial distribution of nutrients at time t=0 depending on the scenario being simulated.

F) Input

Time series of temperature and relative humidity, as well as nutrient levels and distributions, are inputted depending on the scenario being simulated.

G) Submodels

G1) Adjust Climatic Conditions and Bacterial Growth Rates

Temperature and relative humidity are adjusted depending on the scenario being simulated. Potential growth rates of bacteria are calculated as functions of temperature and relative humidity. Maximum potential growth rates, and the associated nutrient requirements, are scaled such that the doubling time of bacteria at 30C and 100% relative humidity with nutrients ad libitum (Ψbase) is ≈ 40 minutes, which is approximately equal to the doubling time of *Bacillus* species under these conditions. Bacterial cells can divide after they have consumed 1 unit of nutrients, thus, at 30C and 100% relative humidity, 0.125 units of nutrients per Δt (per 5-minute time step) are needed to sustain maximum growth. The effect of temperature on growth rate (γ') is demonstrated by Equation 1:

$$\text{Equation 1. } \gamma'(h-1) = (b(T - Tmin))2 * (1 - exp(c(T - Tmin)))$$

where T= current temperature (C, T > 0), Tmin = 3.99 C, Tmax = 43.7 C, b = 0.041, and c = 0.161 (Zwietering et al., 1991). The effect of relative humidity on growth rate (δ) at 30C is demonstrated by Equation 2:

$$\text{Equation 2. } \delta = b0 + b1RH$$

where b0 = 1.725, b1 = 0.043, and RH = relative humidity (%) (Iturriaga et al., 2007).

Assuming Equation 2 holds for 3.99 C < T < 43.7 C, and defining adjusted relative growth rate (δ') as the proportion of the growth rate achieved at 100% RH that is achieved at any given RH, demonstrated by Equation 3:

Equation 3. $\delta' = 0.286307 + 0.007137 * RH$

Thus, growth rate as a function of temperature and relative humidity is demonstrated by Equation 4:

Equation 4. $\gamma\ (h-1) = \delta'((b(T - Tmin))2 * (1 - exp(c(T - Tmax))))$

The associated doubling time (Ψ) is equal to (ln 2) / γ, and the number of units of nutrients per Δt needed to sustain Ψ is equal to 0.125 * (Ψbase / Ψ).

G2) Nutrient Renewal and Plant Root Growth

The spatial distribution of nutrients over the habitat surface and their rate of renewal, as well as root growth rate for those scenarios in which the habitat surface represents as growing plant root, depend on the scenario being simulated.

G3) Plasmid Degradation

Extra-cellular plasmids (plasmids contained by bacteria are released into the surrounding matrix of extra-cellular polymeric substances when bacteria die; under Section G6) have a constant probability of degrading during any given step (Appendix I Table 2).

G4) Spore Formation

Spore formation (metabolically active bacterial cells become metabolically inactive) occurs probabilistically if an active bacterium has been unable to consume nutrients for three consecutive time steps (15 minutes).

G5) Nutrient Consumption

Each active bacterium consumes nutrients from its "nutrient neighborhood," which consists of the 7 x 7 block of 49 habitat cells (18 μm2) centered at the habitat cell in which the bacterium is located (Krone et al., 2007). The bacterium first attempts to consume nutrients from the habitat cell in which it is located. If no nutrients are available, the 8 adjacent cells are

sampled in random order in search of nutrients. If no nutrients are found, the 16 adjacent cells in the next "ring" are sampled in random order, and, finally, the 24 adjacent cells in the next "ring." When a cell with nutrients is encountered, the bacterium consumes the nutrients needed to sustain maximum growth under the current conditions of temperature and relative humidity (= 0.125 * (Ψbase / Ψ), Section G1), or all the nutrients in the cell, whichever is less. A bacterium can consume nutrients from only 1 habitat cell per 5-minute time step. This results implicitly in nutrient diffusion as nutrients are "drawn" from increasingly distant cells within the "nutrient neighborhood."

G6) Death

Bacterial cells die if they have been unable to consume nutrients during 4 consecutive time steps (20 minutes). When bacterial cells die, any plasmids they contain are released into the matrix of extra-cellular polymeric substances in the habitat cell in which they are located (under Section G3).

G7) Reproduction and Segregative Loss

Bacterial cells divide at rates that depend on their consumption and accumulation of nutrients (under Section G5), with the daughter cell placed in a habitat cell within the "growth neighborhood," which consists of the 3 x 3 block of 9 habitat cells (18 μm2) centered at the habitat cell in which the bacterium is located (Krone et al., 2007). If the bacterium has accumulated at least 1 unit of nutrients, it can reproduce (divide), provided there is space available within the growth neighborhood (no habitat cell can contain more than 2 bacteria). If there is space available in the habitat cell in which the bacterium is located, the daughter cell is placed there. If no space is available, the 8 adjacent cells are sampled in random order in search of space. If no available space is found, reproduction is suppressed.

When a plasmid-bearing bacterium reproduces, vertical transmission of plasmids can be complete or incomplete. Segregative loss of plasmids occurs probabilistically (Appendix I Table 2) for each type of plasmid (pXo1, pXo2, pXo16) in each species of bacteria (*B. anthracis, B. cereus, B. thuringiensis*), with the daughter cell containing all or none of the plasmids of the parent cell.

G8) Conjugation

Horizontal transfer of plasmids only occurs between a growing (implicitly elongating) recipient bacterium (Seoane et al., 2010) and a donor bacterium with a mobilizer plasmid (e.g. pXo16; Hu et al., 2009) that is within its growth neighborhood. An active bacterium is defined as "growing" as long as its reproduction has not been suppressed (under Section G7). If there is a bacterium with a pXo16 plasmid in the growth neighborhood, conjugation occurs probabilistically (Appendix I Table 2). If there are two or more potential donor bacteria in the growth neighborhood, one is chosen randomly. If no potential donor bacterium is found, conjugation does not occur. If conjugation occurs, the recipient bacterium also may receive pXo1 and/or pXo2 plasmids from the donor bacterium if the donor bacterium has these plasmids and the recipient bacteria does not already have them (Appendix II Figure 3). The new transconjugant bacterium has a higher probability of transferring the plasmids it has just received than did the donor bacterium, this is, it has a shorter conjugal lag time than the original donor, and the conjugal lag time for transferring a given plasmid continues to decrease with each subsequent conjugation event in which the plasmid is involved (Seoane et al., 2010).

G9) Transformation

Transformation occurs probabilistically (Appendix I Table 2) if there are extra-cellular plasmids in the habitat cell in which a bacterium is located.

G10) Germination

Metabolically inactive bacterial cells germinate (become active) if nutrients become available within their nutrient neighborhood.

CHAPTER III

RESULTS

A) Model Evaluation

A1) Verification of Simulated Patterns of Bacterial Processes

I first evaluated model performance by verifying that simulated patterns of bacterial growth, conjugation and segregative loss, and extra-cellular plasmid transformation and degradation agreed with those reported in the literature upon which I had based model parameterization. I parameterized the effects of temperature and relative humidity on bacterial growth based on the derivations of Zwietering et al. (1991) and the experiments of Iturriaga et al. (2007), respectively. I based my representation of conjugation on the individual-based experiments and computer simulations of plasmid invasion in bacterial populations conducted by Seoane et al. (2010), my parameterization of segregative loss on the estimate of Krone et al. (2007), and my parameterization of transformation extra-cellular plasmid degradation on the data compiled by Lorenz and Wackernagel (1994). Thus, these initial simulations served simply to verify that the various aspects of system dynamics I had parameterized the different parts of the model to reproduce were, in fact, reproduced adequately, and that no obvious inconsistencies had resulted from the integration of the various parts.

A1.1) Growth

To confirm that the model was simulating growth adequately, I initialized the system with one bacterial colony consisting of one bacterium (without plasmids) in each of four adjacent cells in the center of the 5 mm 2 habitat surface, and simulated colony growth over a 24-hour period at various constant temperatures and relative humidities, assuming nutrients were supplied

ad libitum over the entire habitat surface (nutrient renewal rate = 0.125 units per 5-minute time step in each habitat cell). Simulated colony growth at 30˚C and 100% relative humidity essentially filled the habitat surface in 24 hours (Appendix II Figure 4a) with a doubling time during the exponential growth phase ≈ 40 minutes (Appendix II Figure 4b), which was my target base rate for scaling purposes, and also is a reasonable doubling time for a variety of bacterial species (Krone et al., 2007). Simulated colony growth decreased with decreasing temperature in a manner similar to the relationship derived by Zwietering et al. (1991) and with decreasing relative humidity in a manner similar to that observed experimentally by Iturriaga et al. (2007) (Appendix II Figure 4a, 4b).

A1.2) Conjugation and Segregative Loss

To confirm that the model was simulating conjugation and segregative loss adequately, I initialized the system with five bacterial colonies, one in the center and one near each corner of the habitat grid, with each colony again consisting of one bacterium in each of four adjacent cells. Each bacterium in the center (donor) colony contained a conjugative plasmid (pXo16) whereas each bacterium in the four corner (recipient) colonies contained a non-conjugative plasmid (pXo2). I again simulated growth of the colonies over a 24-hour period at 30˚C and 100% relative humidity, assuming nutrients were supplied ad libitum over the entire habitat surface. Simulated numbers of donor and recipient bacteria increased exponentially as they grew toward each other (Appendix II Figures 4c and 5), with the transconjugants appearing shortly after the donor and recipient colonies met after ≈ 7 hours. (Note that a very few transconjugants appeared earlier within the donor colony following segregative loss.) Conjugation occurred slowly as the transfer interface area was forming, accelerated rapidly during a transition phase in which virtually all conjugation events occurred (8 to 12 hours), and essentially ceased thereafter

as the colonies coalesced to occupy all available space, thus suppressing reproduction and conjugation (see Sections G7 and G8). These results corresponded well with the dynamics of plasmid invasion reported by Seoane et al. (2010), who observed conjugation events during an approximately six-hour period after donor and recipient bacterial colonies first began to merge, with plasmids spreading into the recipient colony until conjugation was halted as a result of suppression of further cell growth (cell elongation) in the central portions of the colony due to lack of space. Simulated segregative loss occurred at a rate ≈ 0.005 (data not shown), similar to the estimate of Krone et al. (2007).

A1.3) Transformation and Extra-Cellular Plasmid Degradation

To confirm that the model was simulating transformation and extra-cellular plasmid degradation adequately, I initialized the system with two bacteria and one extra-cellular plasmid in each habitat cell. Bacteria did not contain a plasmid and the extra-cellular plasmids were non-conjugative (pXo2), hence, no conjugative transfer of plasmids was possible. Once again, I simulated system dynamics over a 24-hour period at 30˚C and 100% relative humidity, assuming nutrients were supplied ad libitum over the entire habitat surface. Simulated numbers of transformations increased at a decreasing rate, occurring at a frequency ≈ 0.0004 at first, as observed by Lorenz and Wackernagel (1994), and decreasing in frequency as the number of bacteria without a plasmid decreased (Appendix II Figure 4d). Simulated degradation of extra-cellular plasmids occurred at a frequency ≈ 0.006, as reported by Lorenz and Wackernagel (1994).

A2) Assessment of Simulated Root Surface Colonization and Dynamics

A2.1) Bacterial Colonization of a Homogeneous Root Surface

To assess the ability of the model to simulate bacterial colonization on homogeneous root surfaces, I initialized the system with two bacteria without plasmids in each of 100 randomly-chosen habitat cells (1% of the simulated root surface). I assumed the root occupied the entire habitat surface (5 mm) and that nutrients initially were distributed homogeneously over the entire root surface at a high level (5 nutrient units per root cell). I simulated system dynamics at 30˚C and 100% relative humidity, with no nutrient renewal, until the system had come to a dynamic equilibrium with regard to the numbers of active bacteria (those consuming nutrients), starving bacteria (those still alive but consuming nutrients and having not yet formed spores), and spores. The simulated colonization followed the typical bacterial growth pattern, exhibiting exponential increases in the number of active bacteria, followed by rapid starvation and death or sporulation (Appendix II Figure 6). As bacterial clusters expanded and coalesced, bacteria in the inner portions of larger clusters became isolated from the remaining nutrient patches, entered a starvation phase, and either formed spores or died, thus forming a time-series of mosaic-like patterns of active, starved, and sporulated bacteria. This spatially heterogeneous pattern of root colonization was similar to that reported by Muci et al. (2012), who simulated root surface colonization by bacteria based on laboratory data collected on clover (*Trifolium pratense*) roots using a modeling approach (a combination of cellular automata models and agent-based models) broadly similar to mine. Also, as Muci et al. (2012) noted, such formations of bacterial clusters on root surfaces commonly are observed under natural conditions and usually are attributed to the heterogeneous availability of nutrients in the rhizosphere (Hartmann et al. 2009, Buddrus-Schiemann et al. 2010).

A2.2) Bacterial Colonization of an Elongating Root under Different Nutrient Concentrations

To assess the ability of the model to simulate bacterial colonization on elongating root surfaces with different initial nutrient concentrations, I initialized the system with two bacteria without plasmids in each habitat cell within the upper four rows of the grid, representing the portion of the grid initially occupied by a plant root (within approximately 5.7 μm of the soil surface). I simulated root growth by adding one row of grid cells, moving from the top to the bottom of the grid, after each 5-minute time step (root elongation of approximately 0.41 mm/day). I distributed nutrients homogeneously over the entire initial root surface at either high (5 nutrient units per root cell), medium (3.33 nutrient units per root cell), or low (1.67 nutrient units per root cell) levels, and also initialized each new root cell when it appeared during a simulation with either a high, medium, or low nutrient level, depending on the scenario being simulated. Nutrients were not renewed in existing root cells during the simulations. I simulated system dynamics at 30˚C and 100% relative humidity until the system had come to a dynamic equilibrium with regard to the numbers of active bacteria, starving bacteria, and spores. Under all three scenarios, spores soon outnumbered active bacteria as nutrients on older portions of the root surface were depleted and starved bacteria either formed spores or died (Appendix II Figure 7). The number of bacteria surviving as spores decreased, but the length of time that active bacteria survived on the root surface increased, with decreasing nutrient concentrations. The inverse relationships between nutrient concentration and duration of the presence of active bacteria was due to the inverse relationship between rate of bacterial colonization and length of time nutrients at the newly-forming root tip remained unexploited (beyond the "nutrient neighborhood" of the bacteria at the leading edge of the colonization front). Once again, these patterns were generally similar to those obtained by Muci et al. (2012, Appendix II Figures 3a, 3b) when simulating bacterial colonization of clover roots, and, as these authors noted, such

results are in agreement with the observation that root-colonizing bacteria increase in proportion to the quantities of root exudates (nutrients) released (Hartmann et al. 2009, Buddrus-Schiemann et al. 2010).

A2.3) Bacterial Dynamics in Response to Variable Root Surface Conditions

To assess the ability of the model to simulate bacterial dynamics in response to diurnal and seasonally varying root surface conditions, I initialized the system as described in Section A2.1 and again held temperature at 30˚C and relative humidity at 100%. However, I simulated system dynamics over a 48-hour period with a diurnally pulsing rate of nutrient renewal. Nutrients were renewed simultaneously over the entire root surface at a rate of 0.125 units per 24-hour period. Results were similar to those reported by Muci et al. (2012). I next evaluated model performance under field conditions by examining the sensitivity of simulated bacterial community dynamics to changes in climatic conditions and initial bacterial community composition.

B) Model Demonstration

B1) Establishing a Baseline Simulation Based on Bacterial Proportion

Establishing baseline results for the model, under realistic conditions, was the first step to obtain simulation results. Experimental results published by Raymond et al. (2010) showed that the three bacteria under simulation, *B. anthracis, B. thuringiensis, and B. cereus*, tend to exist in specific proportions within community epiphytically in the wild. While not numerical, Raymond et al. (2010) reported that *B. anthracis* and *B. thuringiensis* exist in much lower quantities compared to *B. cereus*. Using this data, a baseline was established with the goal of finding the lowest proportions of *B. anthracis* and *B. thuringiensis* compared to *B. cereus* possible that would still lead to an outbreak of anthrax spores. An outbreak of anthrax was confirmed after 20

hours of runtime by the simulation by the production of *B. anthracis* spores that contain plasmids pXo1 and pXo2. The confirmed baseline has initial bacterial proportions of 0.5% *B. anthracis*, 1% *B. thuringiensis*, and 98.5% *B. cereus* at standard conditions (30˚C, 100% relative humidity, and other model parameters outlined by Appendix II Table 2). This baseline represents realistic initial proportions for these bacteria in the environment that can potentially generate an incidence case of anthrax poisoning and will be used in further experimentation. Figure 8 (Appendix II) illustrates the temporal dynamics of bacterial conjugation under these baseline conditions, establishing a control for experimental simulations. Transconjugant bacterial levels rose at a steep curve until plateauing around 600 minutes (10 hours) at about 140 bacteria and remaining at those high levels for the remainder of the simulation. Donor bacteria and recipient bacteria exhibited similar patterns in that they both demonstrated a downwards facing parabola, peaking around 305 minutes (about 5 hours). Donor bacteria peaked at a slightly higher level (40 bacteria) compared to recipient bacteria (27 bacteria) before returning to near zero around 645 minutes (10.75 hours).

B2) Experimental Simulation 1: Identifying Temporal Dynamics of the Bacterial Community Assuming B. thuringiensis Cannot Conjugate

In order to investigate whether *B. thuringiensis* is essential in conjugation leading to an outbreak of *B. anthracis* spores, experimental simulation 1 was run in which *B. thuringiensis* could not conjugate. Essentially, any *B. thuringiensis* bacteria within the model could not receive or donate plasmids with genes encoding for anthrax toxins or the protein capsule. Baseline estimates were used to establish this simulation, with initial bacterial proportions kept at 0.5% *B. anthracis*, 1% *B. thuringiensis*, and 98.5% *B. cereus* and standard environmental conditions. A graph demonstrating the temporal dynamics of bacterial conjugation was created and is shown

by Figure 9 (Appendix II). The simulation was run for 20 hours, similarly to the baseline simulation. The same overall pattern is demonstrated by experimental simulation 1 (Appendix II Figure 9) as the baseline (Appendix II Figure 8), within slight differences in that experimental simulation one had slightly lower numbers of transconjugant and donor bacteria. Similarly to the baseline trend, transconjugant bacterial levels rose at a steep curve until plateauing around 600 minutes (10 hours) at about 120 bacteria and remaining at those high levels for the remainder of the simulation. Donor bacteria and recipient bacteria exhibited similar patterns in that they both demonstrated a downwards facing parabola, peaking around 305 minutes (about 5 hours). Donor bacteria peaked at a slightly higher level (21 bacteria) compared to recipient bacteria (26 bacteria) before returning to near zero around 650 minutes (10.83 hours). This is expected, as *B. thuringiensis* could not conjugate, 1% of the initial bacterial population could not engage in conjugation, thus lowering the number of bacteria participating in the donation and transconjugation of plasmids. The rate of production of transconjugant bacteria for each species was established next and is shown by Figure 10 (Appendix II). As the data shows, *B. cereus* was almost the entirety of formed bacterial transconjugants plateauing around 120 bacteria about a third of the way through the simulation, with a very small amount of *B. anthracis* participating in conjugation near the end of the simulation (1-2 bacteria). As *B. thuringiensis* was preset to not be able to conjugate, its rate of transconjugant production remained at zero for the duration of the simulation. Even this limited conjugation between *B. anthracis* and *B. cereus* was enough to produce anthrax spores containing plasmids coding for anthrax toxins near the end of the time frame. Plasmid movement among *B. cereus* adequately allowed for the generation and movement of anthrax related plasmids so that an anthrax outbreak was possible. The final spatial distribution of plasmids is shown by Figure 11 (Appendix II). At the end of the 20 hour period of

the simulation, the majority of all three plasmids, pXo1, pXo2, and pXo16, were present in the extracellular matrix (90% of plasmids), meaning that they were not housed within a bacteria or spore. This data shows that the majority of plasmids were lost from bacteria, through segregative loss, and deposited in the extracellular matrix as the simulation progressed. A small but significant number of plasmids were present in active bacteria (9.9%), and a very small percentage of plasmids were present in spores (0.13%). While a very small amount, this amount represents the 10-15 *B. anthracis* spores, containing the three plasmids, produced by the simulation, signifying an anthrax outbreak. By limiting the conjugation capabilities of *B. thuringiensis*, I have been able to see if *B. thuringiensis* is essential in the production of anthrax spores, which it has proven not to be. While it does contribute to plasmid transfer and spore production in the baseline simulation, these results show it to not be essential. In the absence of *B. thuringiensis* conjugation, *B. cereus* can contribute heavily to conjugation events with *B. anthracis*.

CHAPTER IV

DISCUSSION AND CONCLUSION

Ultimately, I have developed a microscale, agent-based model in order to study anthrax causing *Bacillus* bacteria from a cellular level. Through the first part of the results, model evaluation, I have shown my model functions properly and produces data that is in accordance with natural bacterial behavior. Following model evaluation, the second part of the results was to demonstrate application of the model by establishing a useful baseline and conducting an experimental simulation in which *B. thuringiensis* could not conjugate. The results comprehensively show that this simple, microscale, agent-based model has the capacity to produce results that are compatible with data regarding bacteria behavior from the literature. By understanding the behavior of the bacteria, further experimental simulations can be run in order to make reliable predictions of the causal determinants of an anthrax outbreak.

As discussed in the introduction, previous diagnoses of anthrax inhalation have actually shown to have been caused by *B. cereus* containing plasmids pXo1 and pXo2, not *B. anthracis* (Hoffmaster et al., 2004). The results from experimental simulation 1, particularly data from Figure 10 (Appendix II), showed that despite the lack of conjugation from *B. thuringiensis*, there was adequate conjugation present between *B. cereus* and *B. anthracis* to produce anthrax spores. Environmentally, *B. cereus* has shown the capacity to acquire plasmids necessary for producing an anthrax outbreak, so it is significant that the model not only reflects this but has the capacity to predict this kind of phenomenon. Furthermore, experimental simulation 1 produced only about 10-15 spores, depending on the trial run showing that very small amounts of these *B. anthracis* bacteria are required to produce toxic spores, when able to conjugate with other bacteria in the

Bacillus genus. This model represents only 5mm^2 of plant root surface, so even with very limiting initial proportions, with *B. thuringiensis* not able to conjugate, 10-15 *B. anthracis* spores were produced. When considering the entire root surface area of even one plant (let alone multiple plants), the threshold for minimum required anthrax spores for infection, 2500 (Tessier 2017), can be easily reached. Therefore, the production of any *B. anthracis* spores by this model is enough to constitute an anthrax outbreak.

One limitation, at the moment, of this model is its lack of single-cellular hosts, such as amoebas, on the plant root surface. This model does not incorporate a partial life cycle host, such as an amoeba that can exist epiphytically, particularly in wet areas. The presence of a micro-scale host has shown to increase the production of vegetative *B. anthracis* and ultimately anthrax spores by facilitating the life cycle of *B. anthracis*. Depending on environmental conditions, *B. anthracis* tends to reside in its spore form for long periods of time. This presents an issue related to the conjugation of plasmids, as only vegetative, active bacteria can share DNA. Therefore, *B. anthracis* populations tend to have lower genetic diversity compared to surrounding bacterial populations (Vilas-Bôas et al., 2007). The sharing of the pXo1, pXo2, and pXo16 plasmids is necessary for an anthrax outbreak to occur, so it is evident that another factor could facilitate the life cycle of *B. anthracis*, such as single-celled hosts. Dey et al. (2012) has shown that amoebas, common in moist soils and pools of standing water, serve as amplifiers of *B. anthracis* spores by enabling germination and intracellular multiplication. Therefore, the lack of a host constitutes a limitation to the created environment, on the elongating plant root, that could potentially significantly affect the movement of genetic material between *B. anthracis* bacteria.

Further experimentation will be done using this model. Two interesting directions that show promise for significant impact on this bacterial community comprised of *Bacillus* bacteria

are climate change and nutrient composition. Due to climate change, global temperatures and environmental factors like humidity continuously are shifting. In order to see the effect this might have anthrax-related bacterial temporal dynamics, experimentation will be done in order to identify potential causative environmental factors for these anthrax outbreaks. As mentioned, future directions could also include a detailed study into the nutrient composition of anthrax-infected soils. Within nature, a typical life cycle of *B. anthracis* will include the death of an animal, such as a deer or cow, due to anthrax poisoning after said animal has ingested the bacteria while grazing. As that animal's body decomposes, it feeds the surrounding plants, promoting growth of plants covered in the infectious bacteria. The increased vegetation biomass production found at carcass sites is due to both added nutrients and the proliferation of microbial taxa that can be beneficial for plant growth (Valseth et al., 2017). Thus, future *B. anthracis* transmission events at carcass sites may be indirectly facilitated by the recruitment of plant-beneficial bacteria (Valseth et al., 2017). Therefore, varying levels of nutrient composition play a significant role in the life cycle of *B. anthracis* and the production of anthrax outbreaks environmentally, so further investigation through this model is necessary.

REFERENCES

Abedon, S. T., Herschler, T. D., and Stopar, D., 2001. Bacteriophage latent-period evolution as a response to resource availability. Appl. Environ. Microbiol., 67:4233-4241.

Akhtar, P. and Khan, S.A., 2012. Two independent replicons can support replication of the anthrax toxin-encoding plasmid pXO1 of Bacillus anthracis. Plasmid, 67(2):111-117.

Bahl, M.I. and Rosenberg, K., 2010. High abundance and diversity of *Bacillus anthracis* plasmid pXO1-like replicons in municipal wastewater. FEMS Microbiol. Ecol., 74(1):241-247.

Barro A. S., Fegan M., Moloney B., Porter K., Muller J., Warner S., Blackburn J. K., 2016. Redefining the Australian Anthrax Belt: Modeling the Ecological Niche and Predicting the Geographic Distribution of Bacillus anthracis. PLOS Neglected Tropical Diseases 10(6): e0004689.

Birge, E.A., 2013. Bacterial and bacteriophage genetics 3rd edition. Springer-Verlag, New York.

Blackburn J. K., 2006. Evaluating the spatial ecology of Anthrax in North America: examining epidemiological components across multiple geographic scales using a GIS-based approach, Louisiana State University, Baton Rouge, LA.

Blackburn J. K., Matakarimov S., Kozhokeeva S., Tagaeva Z., Bell L. K., Kracalik I. T., Zhunushov, 2017. Modeling the Ecological Niche of Bacillus anthracis to Map Anthrax Risk in Kyrgyzstan. Am J Trop Med Hyg.: 96(3): 550–556.

Brehm-Stecher, B.F. and Johnson, E. A., 2004. Single-cell microbiology: tools, technologies, and applications. Microbiol. Mol. Biol. Rev., 68:538-559.

Buddrus-Schiemann K., Schmid M., Schreiner K., Welzl G., Hartmann A., 2010. Root Colonization by Pseudomonas sp. DSMZ 13134 and Impact on the Indigenous Rhizosphere Bacterial Community of Barley. Microbial Ecology, 60:381-393.

Carroll L.M., Wiedmann M., Kovac J., 2019. Proposal of a taxonomic nomenclature for the *Bacillus cereus* group which reconciles genomic definitions of bacterial species with clinical and industrial phenotypes. bioRxiv 779199.

Czárán T. and Hoekstra R. F., 2009. Microbial communication, cooperation and cheating: quorum sensing drives the evolution of cooperation in bacteria. PLoS ONE, 4:e6655.

Dey R., Hoffman P. S., Glomski I. J., 2012. Germination and amplification of anthrax spores by soil-dwelling amoebas. Appl Environ Microbiol, 78(22):8075-81.

Dionisio, F., Matic, I., Radman, M., Rodrigues, O.R., Taddei, F., 2002. Plasmids Spread Very Fast in Heterogeneous Bacterial Communities. Genetics, 162(4):1525-1532.

Evans, T., Bowers, R. G., and Mortimer, M., 2007. Modelling the stability of Stx lysogens. Journal of Theoretical Biology, 248:241-250.

Faust K., Sathirapongsasuti J.F., Izard J., Segata N., Gevers D., Raes J., Huttenhower C., 2012. Microbial Co-occurrence Relationships in the Human Microbiome. PLOS Computational Biology 8(7): e1002606.

Gauvry, E., Mathot A-G., Couvert O., Leguérinel I., Jules M., Coroller L., 2019. Differentiation of Vegetative Cells into Spores: a Kinetic Model Applied to *Bacillus subtilis*. Applied and Environmental Microbiology 85(10): e00322-19.

Goel A. K., 2015. Anthrax: A disease of biowarfare and public health importance. World journal of clinical cases, 3(1): 20–33.

Granter, S.R., Bernstein, A., Ostfeld, R.S., 2014. Of mice and men: lyme disease and biodiversity. Perspect. Biol. Med., 57(2):198-207.

Gregory, R., Saunders, J. R., and Saunders, V. A., 2008. Rule-based modelling of conjugative plasmid transfer and incompatibility. Biosystems, 91:201-215.

Gregory, R., Saunders, V. A., and Saunders, J. R., 2010. Rule-based modelling of conjugative plasmid transfer and incompatibility. Biosystems, 91:201-215.

Grimm, V., Berger, U., Bastiansen, F., Eliassen, S., Ginot, V., Giske, J., Goss-Custard, J., Grand, T., Heinz, S. K., Huse, G., Huth, A., Jepsen, J. U., Jørgensen, C., Mooij, W. M., Müller, B., Pe'er, G., Piou, C., Railsback, S. F., Robbins, A. M., Robbins, M. M., Rossmanith, E., Rüger, N., Strand, E., Souissi, S., Stillman, R. A., Vabø, R., Visser, U., and DeAngelis, D. L., 2006. A standard protocol for describing individual-based and agent-based models. Ecological Modelling, 198:115-126.

Grimm, V. and Railsback, S. F., 2005. Individual-based modeling and ecology. Princeton University Press, Princeton, NJ, 428 p.

Hartmann A., Schmid M., van Tuinen D., Berg G., 2008. Plant-driven selection of microbes. Plant and Soil, 321:235-257.

Helgason, E., Okstad, O.A., Caugant, D.A., Johansen, H.A., Fouet, A., Mock, M., Hegna, I. and Kolsto, A.B., 2000. *Bacillus anthracis, Bacillus cereus,* and *Bacillus thuringiensis* – one species on the basis of genetic evidence. Appl. Environ. Microbiol., 66:2627-2630.

Hinnekens, P., Koné K.M., Fayad N., Leprince A., Mahillon J., 2019. pXO16, the large conjugative plasmid from *Bacillus thuringiensis* serovar *israelensis* displays an extended host spectrum. Plasmid, 102:46-50.

Hoffmaster, A.R., Ravel, J., Rasko, D.A., Chapman, G.D., Chute, M.D., Marston, C.K., De, B.K., Sacchi, C.T., Fitzgerald, C., Mayer, L.W., Maiden, M.C.J., Priest, F.G., Barker, M., Jiang, L., Cer, R.Z., Rilstone, J., Peterson, S.N., Weyant, R.S., Galloway, D.R., Read, T.D., Popovic, T. and Fraser, C.M., 2004. Identification of anthrax toxin genes in a *Bacillus cereus* associated with an illness resembling inhalation anthrax. Proceedings of the National Academy of Sciences of the United States of America, 101:8449-8454.

Hu, X., Van der Auwera, G., Timmery, S., Zhu, L. and Mahillon, J., 2009. Distribution, diversity, and potential mobility of extrachromosomal elements related to the *Bacillus anthracis* pXO1 and pXO2 virulence plasmids. Appl. Environ. Microbiol., 75:3016-3028.

Iturriaga, M.H., Tamplin, M.L., and Escartin, E.F., 2007. Colonization of tomatoes by *Salmonella montevideo* is affected by relative humidity and storage temperature. Journal of Food Protection, 70:30-34.

Keesing, F., Belden, L.K., Daszak, P., Dobson, A., Harvell, C.D., Holt, R.D., Hudson, P., Jolles, A., Jones, K.E., Mitchell, C.E., Meyers, S.S., Bogich, T., and Ostfeld, R.S., 2010. Impacts of biodiversity on the emergence and transmission of infectious diseases. Nature, 468:647-652.

Kiel J., Walker W.W., Andrews C.J., Santos A.D.L., Adams R.N., Bucholz M.W., McBurnett S.D., Fuentes V., Rizner K.E., and Blount K.W., 2009. Pathogenic ecology: where have all the pathogens gone? Anthrax: a classic case. Chemical, Biological, Radiological, Nuclear, and Explosives (CBRNE) Sensing X. SPIE, Orlando, FL, USA, pp. 730402-730409.

Kolter, R., 2010. Biofilms in lab and nature: a molecular geneticist's voyage to microbial ecology. Int Microbiol., 13:1-7.

Kreft, J.U., Booth, G. and Wimpenny, J.W.T., 1998. BacSim, a simulator for individual-based modelling of bacterial colony growth. Microbiology, 144:3275-3287.

Krone, S.M., Lu, R., Fox, R., Suzuki, H., and Top, E.M., 2007. Modelling the spatial dynamics of plasmid transfer and persistence. Microbiology, 153:2803-2816.

Laschov, D. and Margaliot, M., 2009. Mathematical modelling of the lambda switch: a fuzzy logic approach. Journal of Theoretical Biology, 260:475-489.

LoGiudice, K., Ostfeld, R.S., Schmidt, K.A., and Keesing, F., 2003. The ecology of infectious disease: effects of host diversity and community composition on Lyme disease risk. Proceedings of the National Academy of Sciences of the United States of America, 100:567-571.

Lorenz, M.G. and Wackernagel, W., 1994. Bacterial gene transfer by natural genetic transformation in the environment. Microbiol. Mol. Biol. Rev., 58:563-602.

Maloy, S.R., Cronan, J.E.J., and Freifelfer, D. L., 1994. Microbial genetics. Jones & Bartlett, Boston.

Muci A.L., Jorquera M.A., Ávila Á.I., Rengel Z., Crowley D.E., Mora M.,
2012. A combination of cellular automata and agent-based models for simulating the root surface colonization by bacteria. Ecological Modelling, 247:1-10.

Normander, B., Christensen, B.B., Molin, S., and Kroer, N., 1998. Effect of bacterial distribution and activity on conjugal gene transfer on the phylloplane of the bush bean (*Phaseolus vulgaris*). Appl. Environ. Microbiol., 64:1902-1909.

Okinaka, R., Cloud, K., Hampton, O., Hoffmaster, A., Hill, K., Keim, P., Koehler, T., Lamke, G., Kumano, S., Manter, D., Martinez, Y., Ricke, D., Svensson, R., and Jackson, P., 1999. Sequence, assembly, and analysis of pXo1 and pXo2. Journal of Applied Microbiology, 87:261-262.

Payne, R. J. H. and Jansen, V. A. A., 2001. Understanding bacteriophage therapy as a density-dependent kinetic process. Journal of Theoretical Biology, 208:37-48.

Pena-Gonzalez A., Rodriguez-R L.M., Marston C.K., Gee J.E., Gulvik C.A., Kolton C.B., Saile E., Frace M., Hoffmaster A.R., Konstantinidis K.T., 2018. Genomic Characterization and Copy Number Variation of *Bacillus anthracis* Plasmids pXO1 and pXO2 in a Historical Collection of 412 Strains. mSystems, 3(4): e00065-18.

Raymond B., Wyres K.L., Sheppard S.K., Ellis R.J., Bonsall M.B., 2010. Environmental Factors Determining the Epidemiology and Population Genetic Structure of the *Bacillus cereus* Group in the Field. PLoS Pathog, 6(5): e1000905.

Reddy, A., Battisti, L., and Thorne, C.B., 1987. Identification of self-transmissible plasmids in four *Bacillus thuringiensis* subspecies. J. Bacteriol., 169:5263-5270.

Saile E. and Koehler T. M., 2006. *Bacillus anthracis* multiplication, persistence, and genetic exchange in the rhizosphere of grass plants. Appl. Environ. Microbiol., 72:3168-3174.

Salkeld, D.J., Salathé M., Stapp P., and Jones J. H., 2010. Plague outbreaks in prairie dog populations explained by percolation thresholds of alternate host abundance. Proceedings of the National Academy of Sciences.

Schwartz, M., 2009. Dr. Jekyll and Mr. Hyde: A short history of anthrax. Elsevier Molecular Aspects of Medicine, 30(6):347-355.

Schuch, R., Nelson, D., and Fischetti, V. A., 2002. A bacteriolytic agent that detects and kills *Bacillus anthracis*. Nature, 418:884-889.

Seoane, J., Yankelevich, T., Dechesne A., Merkey B., Sternberg C., Smets B. F., 2010a. An individual-based approach to explain plasmid invasion in bacterial populations. FEMS Microbiology Ecology, 75(1):17-27.

Seoane, J. M., 2010b. Individual-based analysis and prediction of the fate of plasmids in spatially structured bacterial populations. Kgs. Lyngby, Denmark: Technical University of Denmark (DTU).

Sharma, S., Gopu, V., Sivasankar, C., Shetty, P. H., 2019. Hydrocinnamic acid produced by *Enterobacter xiangfangensis* impairs AHL-based quorum sensing and biofilm formation in *Pseudomonas aeruginosa*. RSC Advances, 9:28678-28687.

Sonenshine, D.E. and Mather, T. N., 1994. Stability and conjugal transfer kinetics of a TOL plasmid in *Pseudomonas aeruginosa* PAO 1162. FEMS Microbiology Ecology, 15:337-350.

Taylor-Joyce, G., Brooker, T., Waterfield, N., 2019. The impact of a horizontally acquired virulence plasmid on Bacillus cereus G9241, the causative agent of an anthrax-like illness. Access Microbiology, 1(1A):po0541.

Tessier, J., 2017. Anthrax and Microbiology of *B. anthracis*. In Infectious Disease Advisor. Retrieved from https://www.infectiousdiseaseadvisor.com/home/decision-support-in-medicine/infectious-diseases/anthrax-and-microbiology-of-b-anthracis/.

Valseth K., Nesbø C. L., Easterday W. R., Turner W. C., Olsen J. S., Stenseth N. C., Haverkamp T. H. A., 2017. Temporal dynamics in microbial soil communities at anthrax carcass sites. BMC Microbiol., 17(1):206.

Vilas-Bôas G. T., Peruca A. P. S, Arantes O. M. N, 2007. Biology and taxonomy of Bacillus cereus, Bacillus anthracis, and Bacillus thuringiensis. Canadian Journal of Microbiology, 53(6):673-687.

Vlachos, C., Paton, R. C., Saunders, J. R., and Wu, Q. H., 2006. A rule-based approach to the modelling of bacterial ecosystems. Biosystems, 84:49-72.

Wei, W. and Krone, S.M., 2005. Spatial invasion by a mutant pathogen. Journal of Theoretical Biology, 236:335-348.

Wood, T. K., Hong, S. H., and Ma, Q., 2010. Engineering biofilm formation and dispersal. Trends in Biotechnology, 29:87-94.

Zwietering, M.H., de Koos, J.T., Hasenack, B.E., de Witt, J.C., and van't Riet, K., 1991. Modeling of bacterial growth as a function of temperature. Appl. Environ. Microbiol., 57:1094-1101.

APPENDIX I

TABLES

Table 1. (a) State variables characterizing low-level model entities.

	State Variables	Category or Value/Unit
Habitat Cells	Identification Number	ID # of habitat cell
	Location	X and Y coordinates indicating position within the grid
	Plant root in cell?	Yes or No
	Nutrient Level	# of arbitrary units
	Rate of Nutrient Renewal	# arbitrary units per 5 minutes
Bacteria	Identification Number	ID # of bacteria
	Species	*B. anthracis, B. thuringiensis,* or *B. cereus*
	State	Active or Spore
	Nutrient Requirement	Number of units of nutrients required per 5 minutes to grow at maximum rate
	Nutrients Consumed	Number of units of nutrients accumulated since last cell division
	Accumulated Nutrients	Number of units of nutrients accumulated since last reproduction (cell division)
	Starvation Level	Number of consecutive 5-minute periods in which no consumption has occurred
	Identification number of Xo1 and plasmid within the cell	ID # of Xo1 plasmid, if present
	Identification number of Xo2 plasmid within the cell	ID # of Xo2 plasmid, if present
	Identification number of Xo16 plasmid within the cell	ID # of Xo16 plasmid, if present
Plasmids	Identification Number	ID # of plasmid
	Kind	Xo1, Xo2, or Xo16
	In Bacteria	ID # of bacterium in which located or "-1" if not in bacterium
	State	Active or in Spore
	Conjugation Events	# of conjugation events to date

Table 1. (b) Auxiliary variables characterizing aggregated model entities.

Auxiliary Variable
Number of active bacterial cells in system
Number of inactive bacterial cells (spores) in system
Number of active *B. anthracis* cells in system
Number of active *B. thuringiensis* cells in system
Number of active *B. cereus* cells in system
Number of *B. anthracis* spore cells in system
Number of *B. thuringiensis* spore cells in system
Number of *B. cereus* spore cells in system
Number of Xo1 plasmids in system
Number of Xo2 plasmids in system
Number of Xo16 plasmids in system
Number of Xo1 plasmids in active bacteria
Number of Xo2 plasmids in active bacteria
Number of Xo16 plasmids in active bacteria
Number of Xo1 plasmids in spores
Number of Xo2 plasmids in spores
Number of Xo16 plasmids in spores
Number of Xo1 extra-cellular plasmids
Number of Xo2 extra-cellular plasmids
Number of Xo16 extra-cellular plasmids

Table 2. Values of model parameters.

Parameter	Value	Unit	Reference
Doubling time (base rate at 30C, relative humidity = 100%; same for all bacteria)	40	Minutes	Krone et al., 2007
Plasmid degradation rate (same for all plasmids)	0.006	Probability (≈15 hour half-life)	Lorenz and Wackernagel, 1994
Spore Formation	0.5	Probability	Gauvry et al., 2009
Segregative Loss Rate (same for all plasmids in all bacteria)	0.005	Probability	Krone et al., 2007
Conjugation rate (base rate same for all donor bacteria)	0.05	Probability	Seoane et al., 2010
First transconjugant conjugation rate (same for all bacteria)	3	Multiple of base rate	Seoane et al., 2010
Second, third, etc. transconjugant conjugation rate (same for all bacteria)	16	Multiple of base rate	Seoane et al., 2010
Transformation rate (same for all bacteria and extra-cellular plasmids)	0.0004	Probability	Lorenz and Wackernagel, 1994

Note: Values expressed as probabilities represent probability of occurrence at the individual level (bacterium or plasmid) per 5 minutes.

APPENDIX II

FIGURES

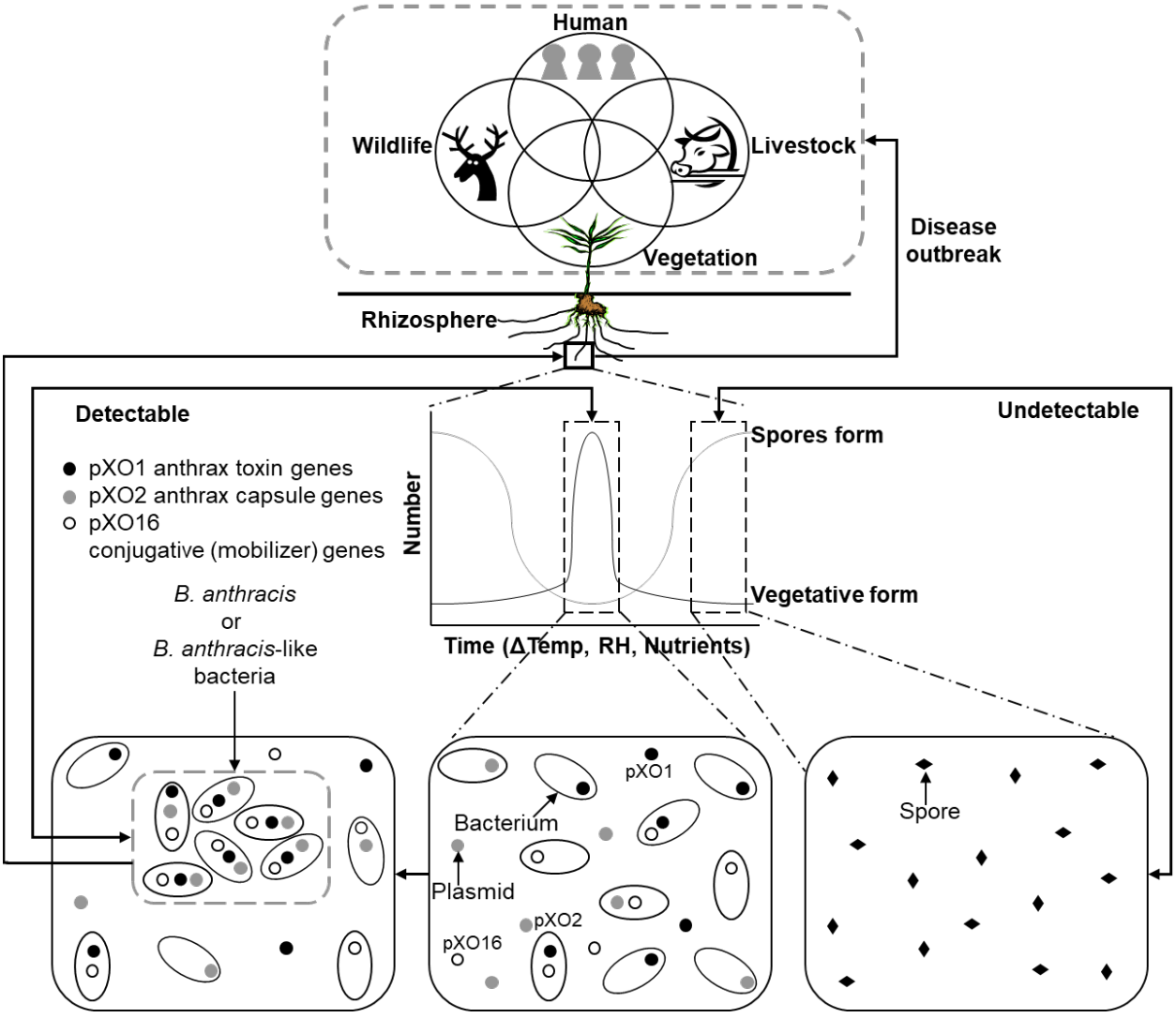

Figure 1. Conceptualization of the spatial-temporal dynamics of bacterial communities composed of *Bacillus* species and the surrounding matrix of extra-cellular polymeric substances on the surface of a hypothetical plant root, and their potential role in disease outbreaks.

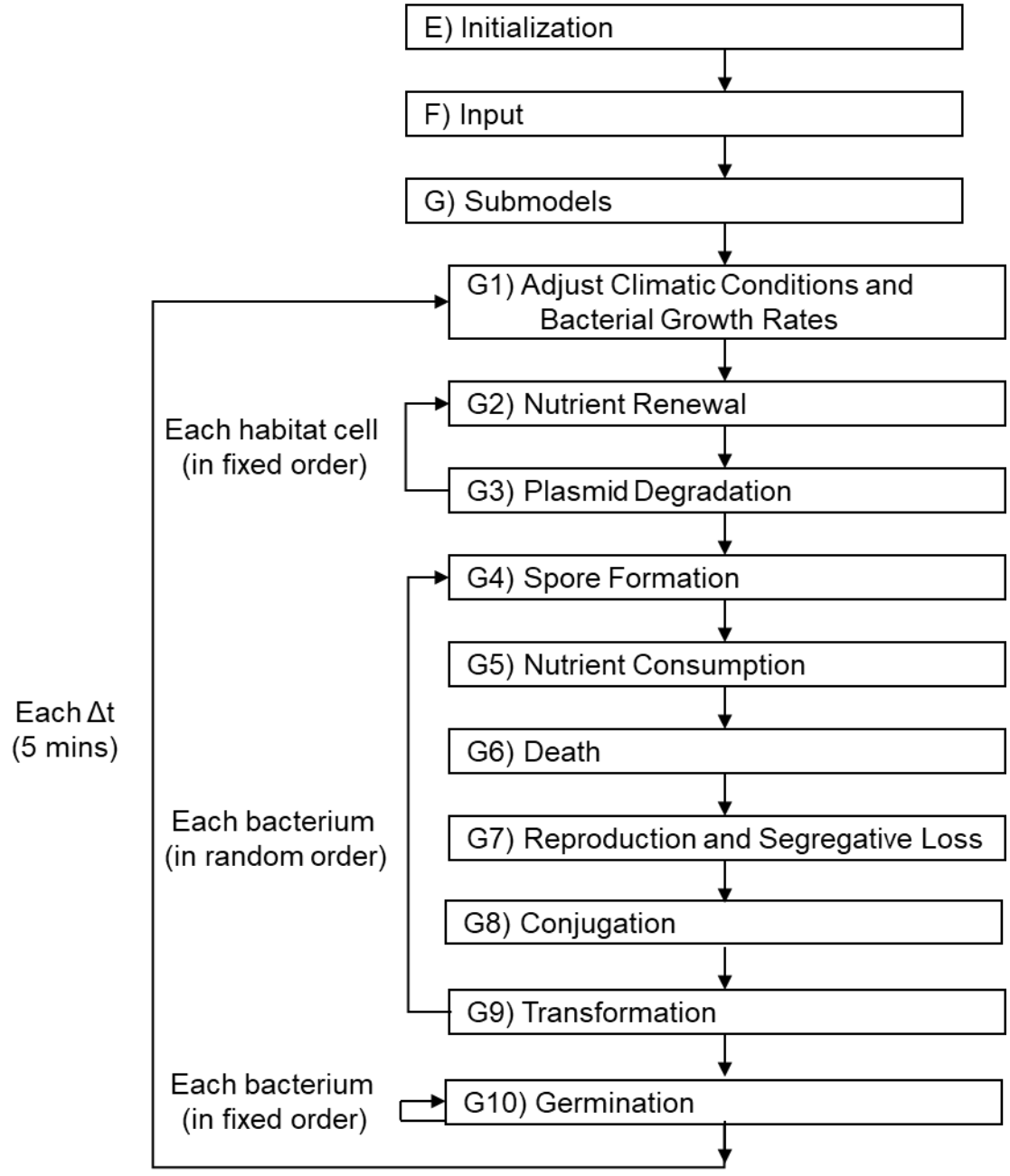

Figure 2. Overview of the scheduling processes and calculations during execution of the model.

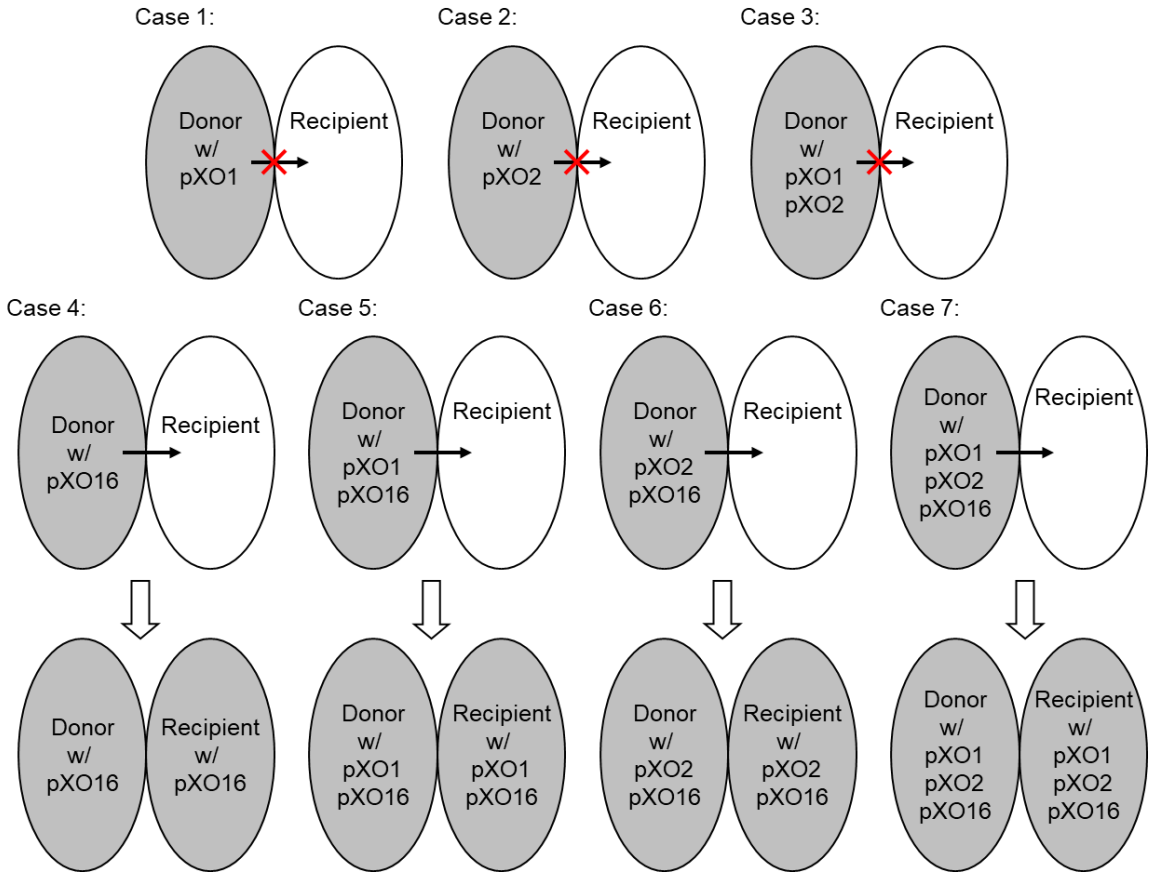

Figure 3. Diagrammatic representation of the horizontal transfer of plasmids via bacterial conjugation. Horizontal transfer only occurs between a growing recipient bacterium and a donor bacterium with a mobilizer plasmid (Xo16). If conjugation occurs, the recipient bacterium receives all of the plasmids from the donor bacterium that it does not already have.

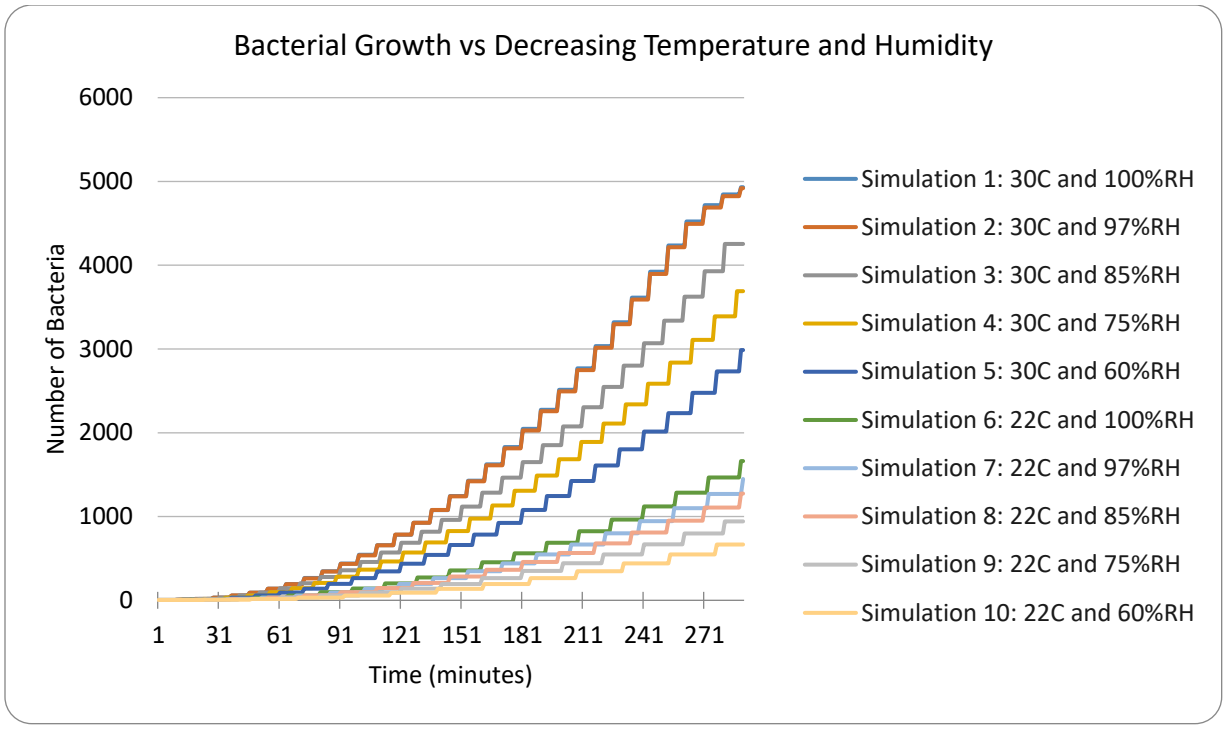

Figure 4a. Results of simulation evaluating temporal patterns of bacterial growth at decreasing temperatures and relative humidity, produced by the model.

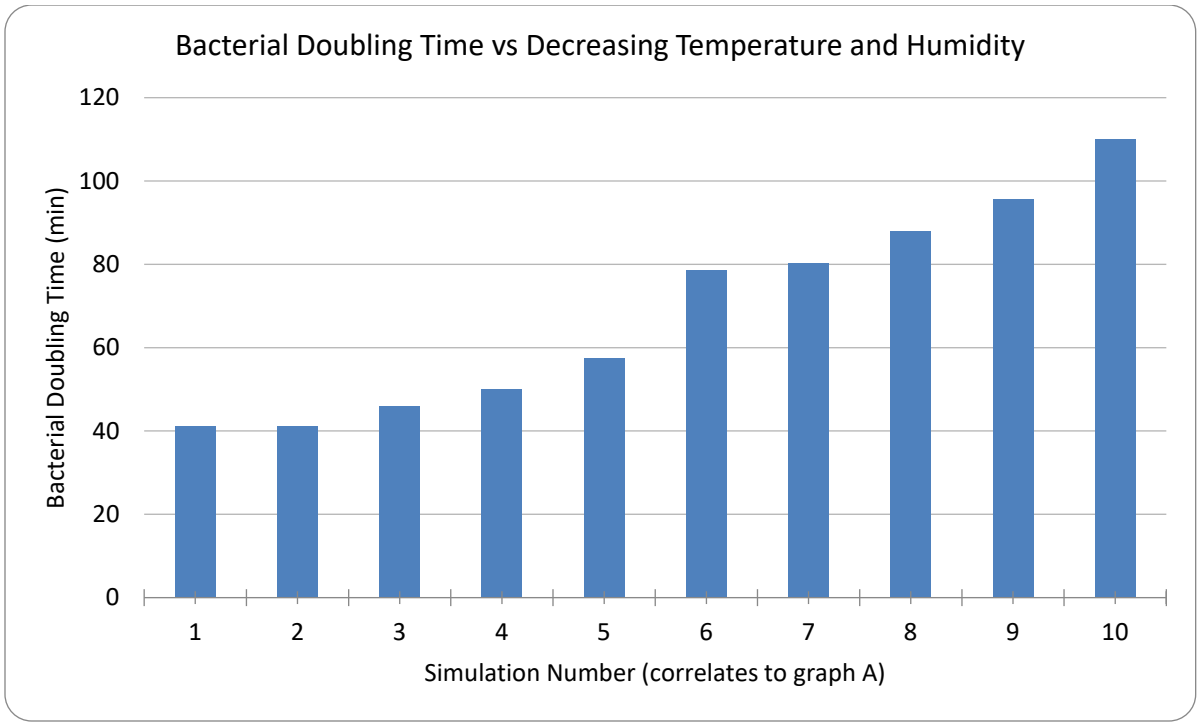

Figure 4b. Results of simulations evaluating associated doubling times for the same simulations as Figure 4a, produced by the model.

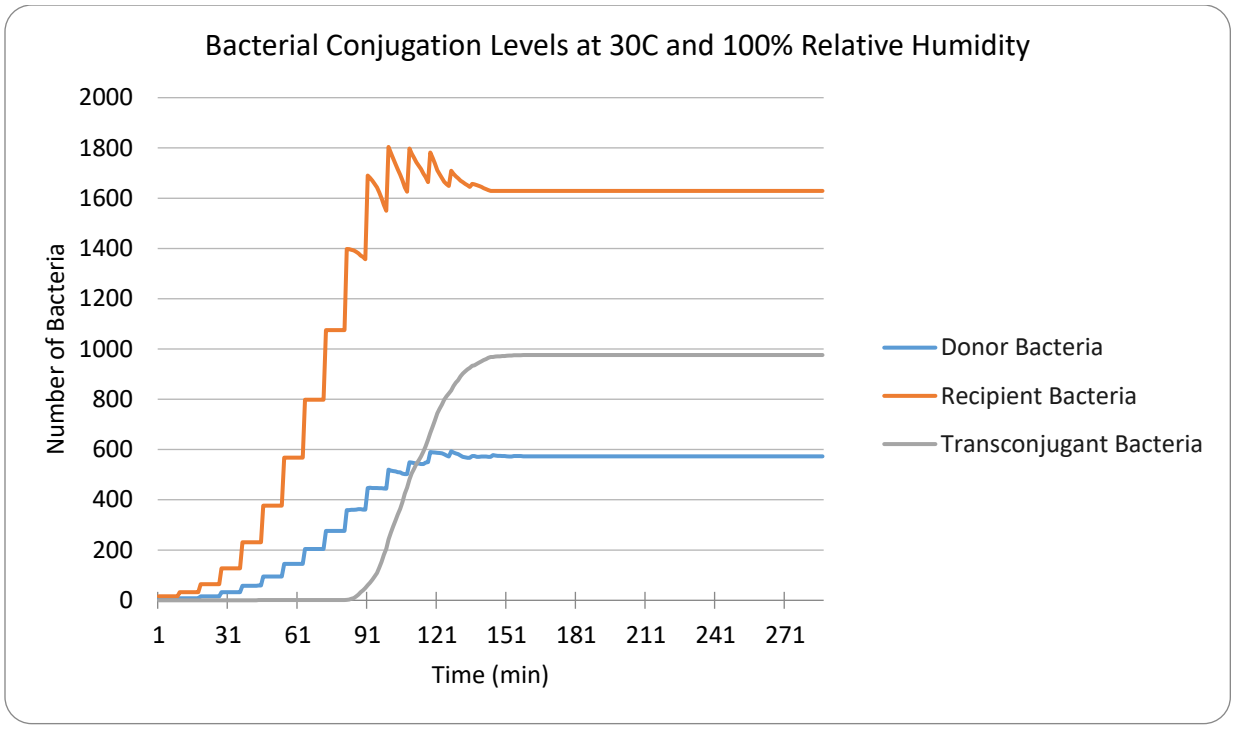

Figure 4c. Results of simulations evaluating conjugation and segregative loss rates at 30˚C and 100% relative humidity, produced by the model.

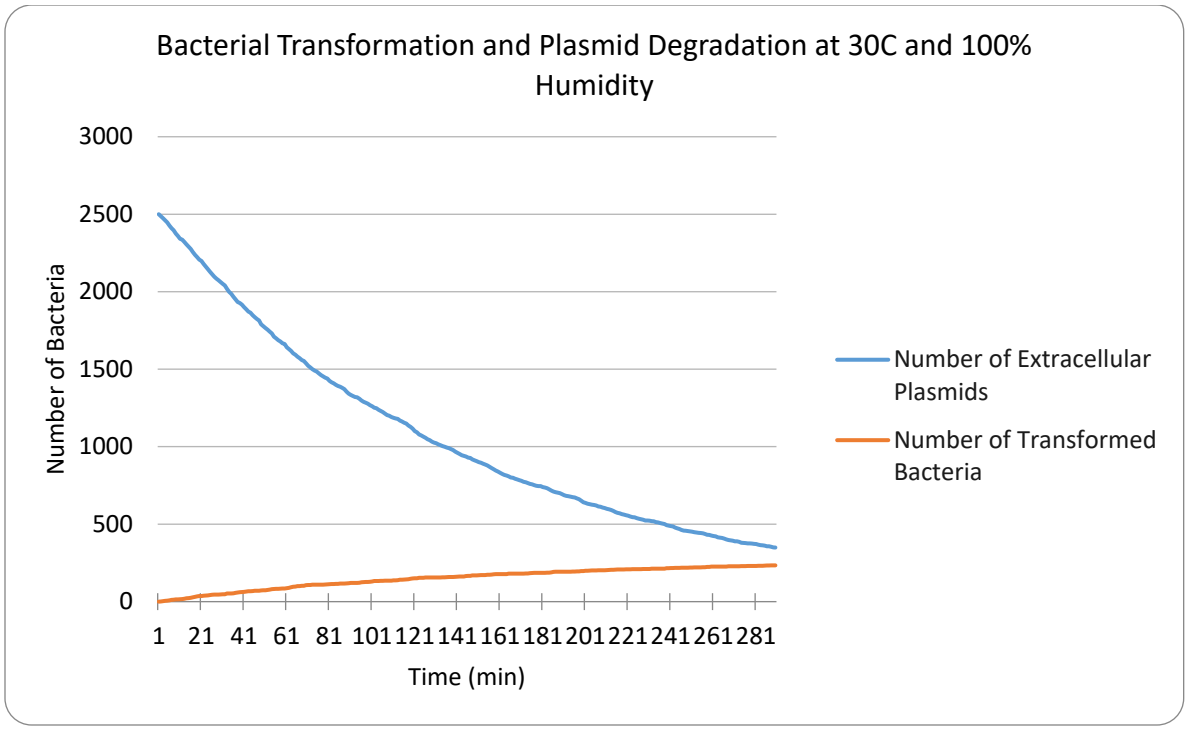

Figure 4d. Results of simulations evaluating transformation and degradation of extra-cellular plasmids at 30˚C and 100% relative humidity, produced by the model.

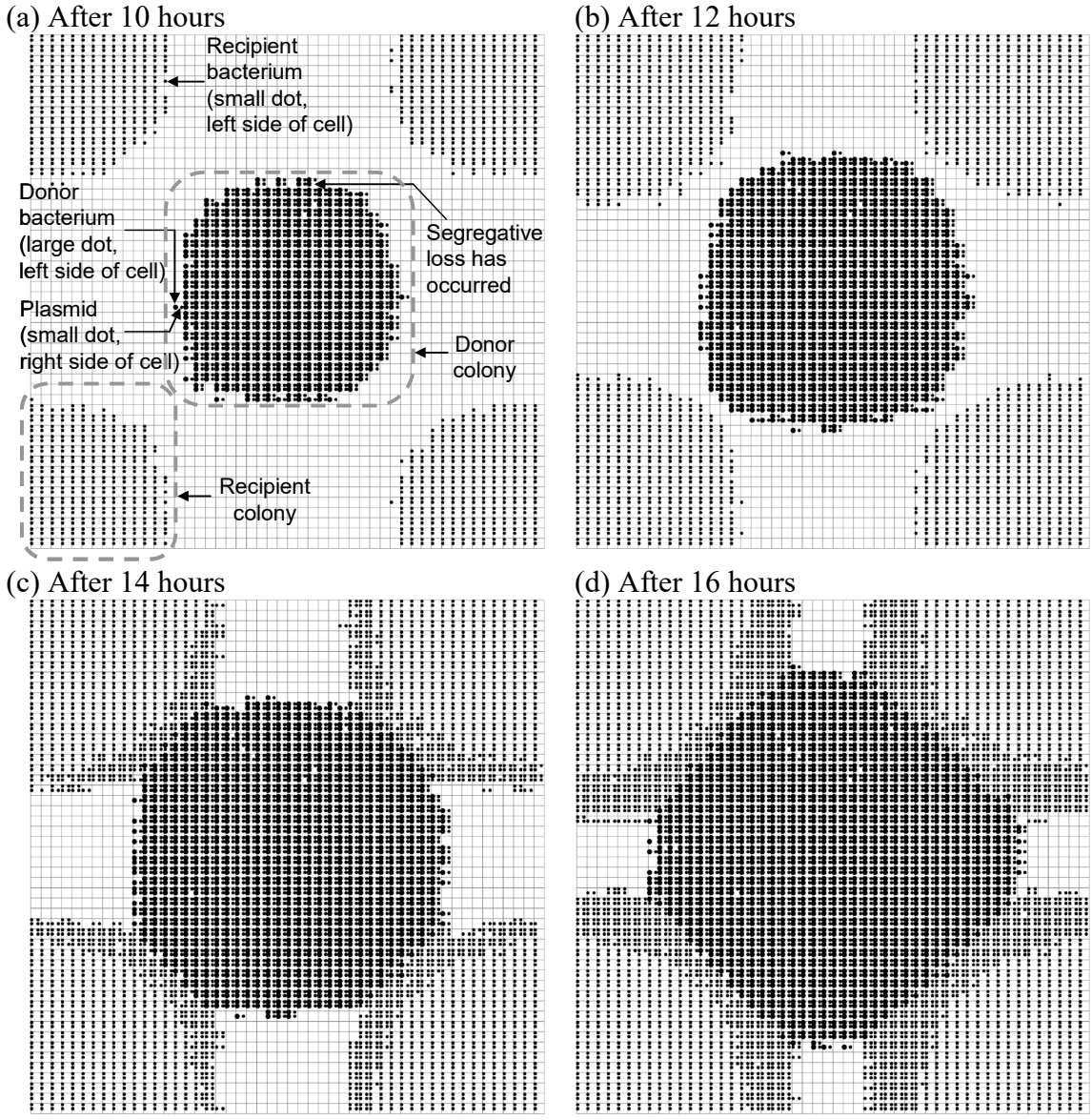

Figure 5a-d. Results of simulations evaluating spatial patterns of bacterial conjugation and plasmid invasion of recipient colonies at 30˚C and 100% relative humidity. As labeled in section A, donor bacteria are labeled as a large dot on the left side of the cell, recipient bacteria are labeled as a small dot on the left side of the cell, and plasmids are labeled as a small dot on the right side of the cell.

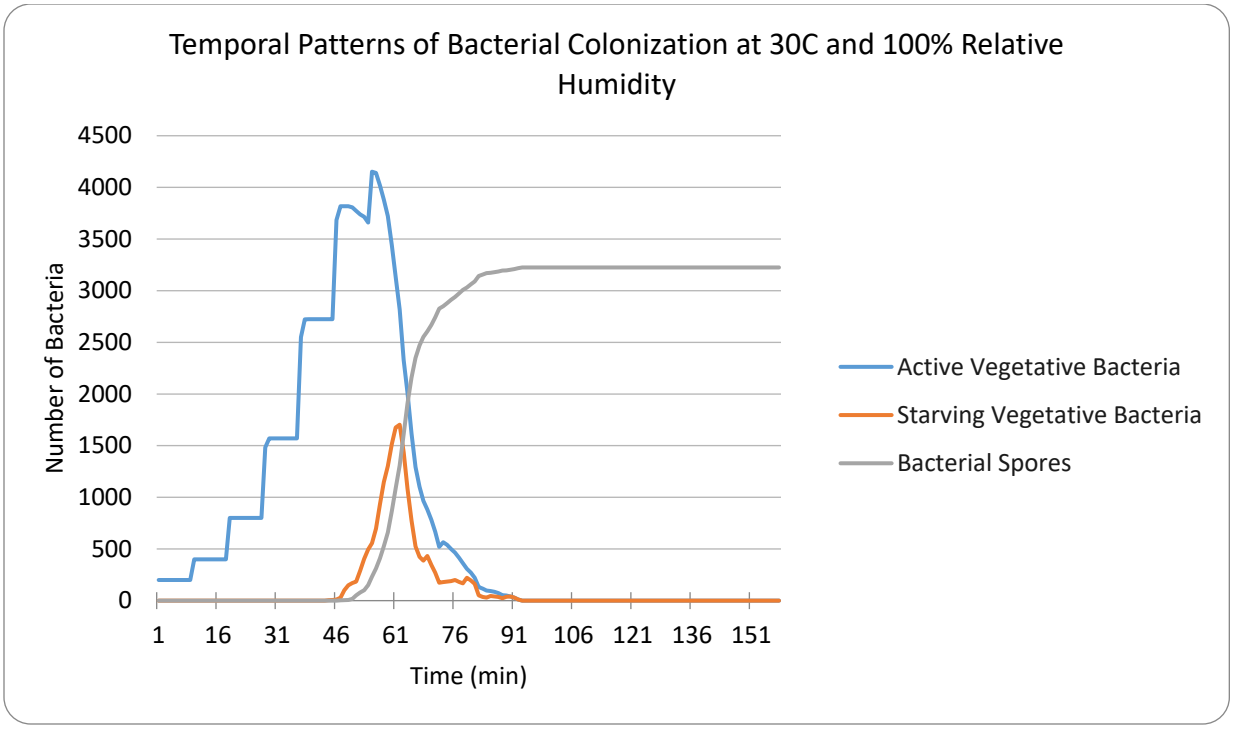

Figure 6. Results of simulations evaluating temporal patterns of bacterial colonization (numbers of active vegetative bacteria, starving vegetative bacteria, and bacterial spores) on homogeneous root surfaces with high initial concentrations under conditions of 30˚C and 100% relative humidity.

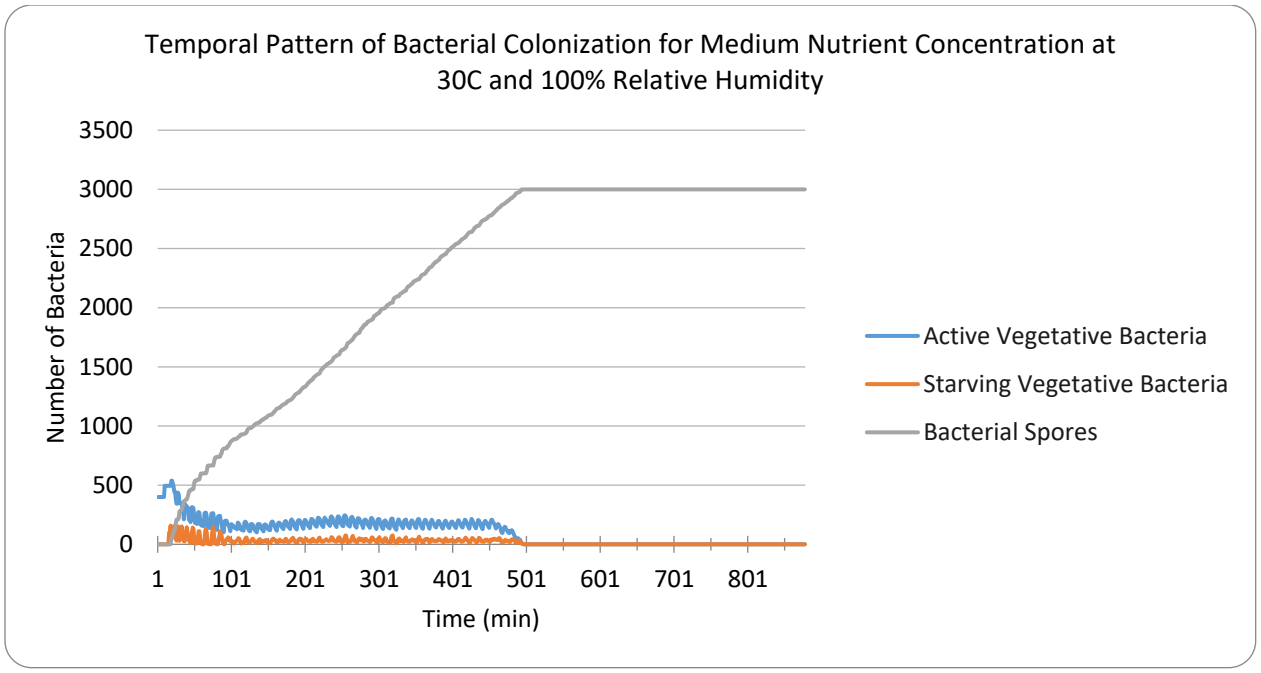

Figure 7a. High Nutrient Concentration.

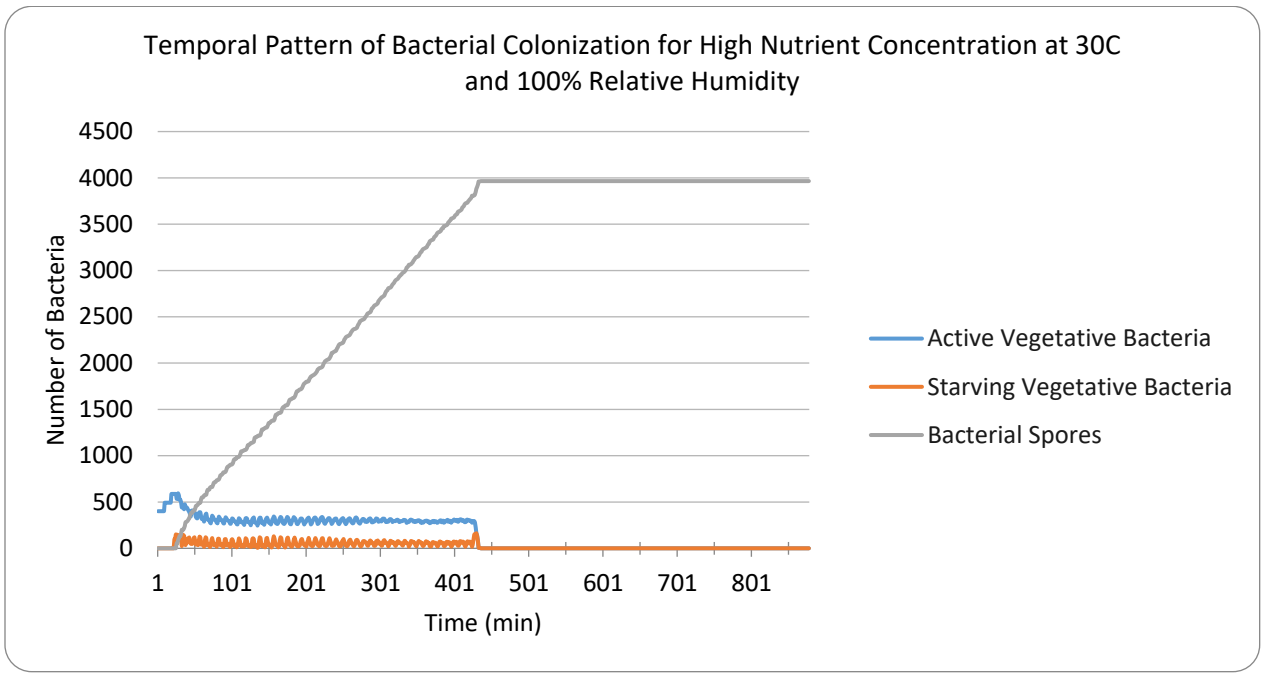

Figure 7b. Medium Nutrient Concentration

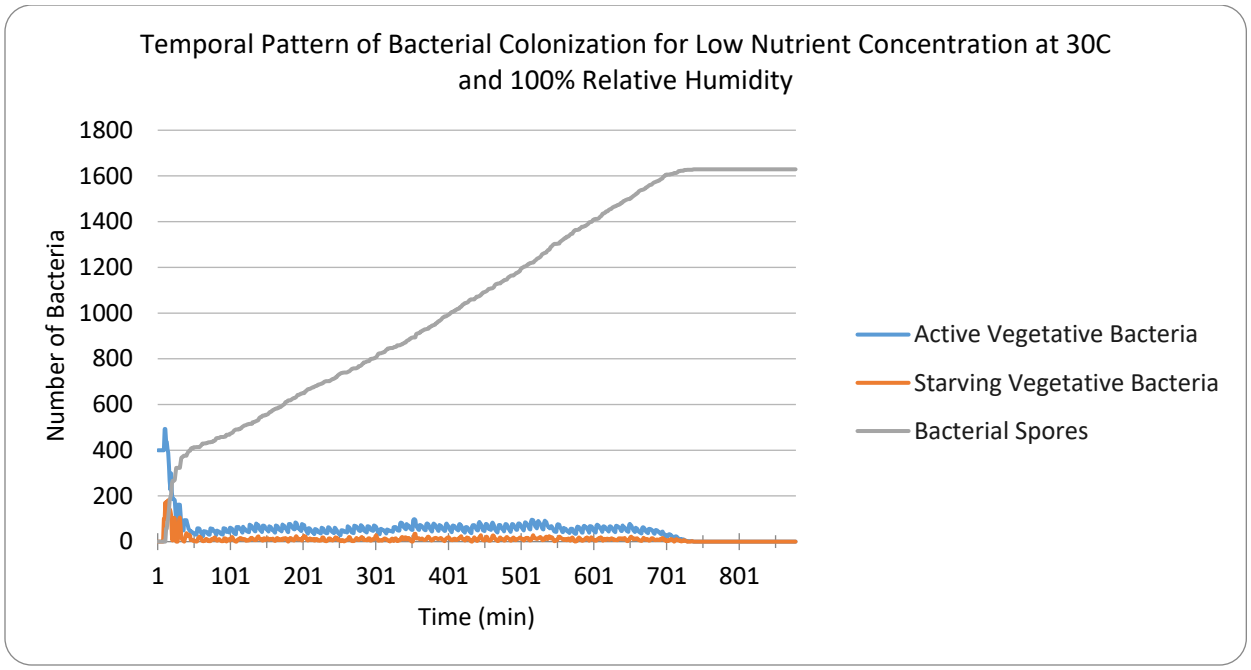

Figure 7c. Low Nutrient Concentration.

Figure 7a-c. Results of simulations evaluating temporal patterns of bacterial colonization (number of active vegetative bacteria, starving vegetative bacteria, and bacterial spores) on elongating root surfaces with (a) high, (b) medium, and (c) low initial nutrient concentrations under conditions of 30˚C and 100% relative humidity.

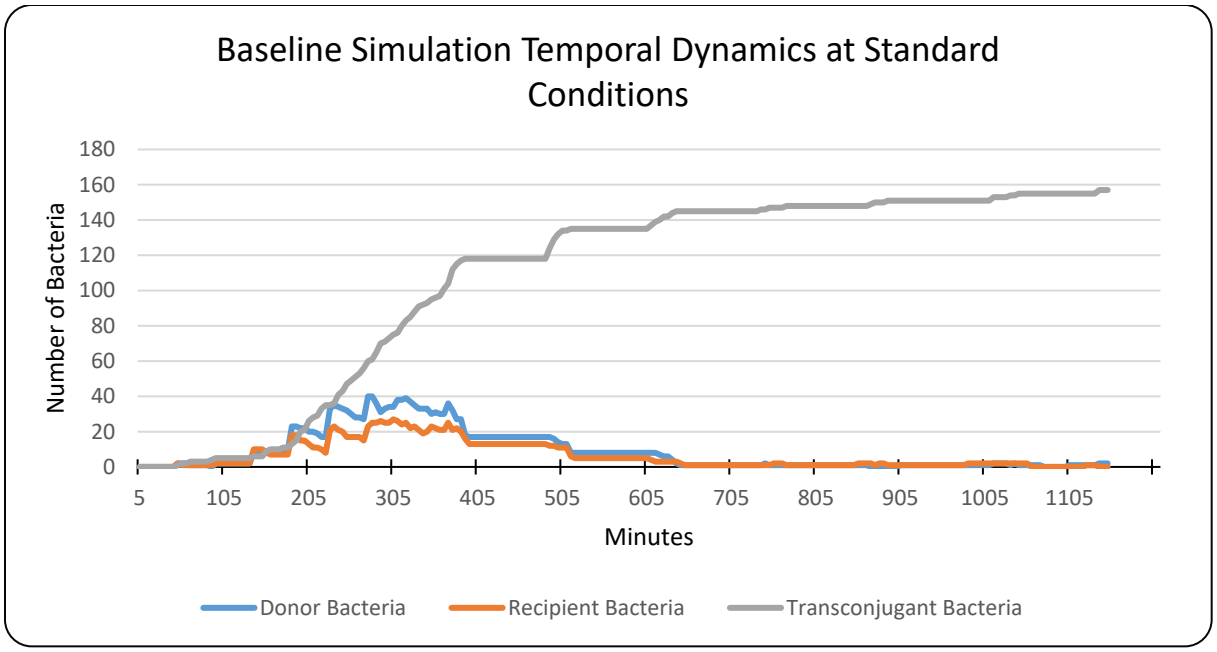

Figure 8. Results of baseline simulation establishing control for bacterial conjugation temporal dynamics on elongating root surfaces under conditions of 30˚C and 100% relative humidity.

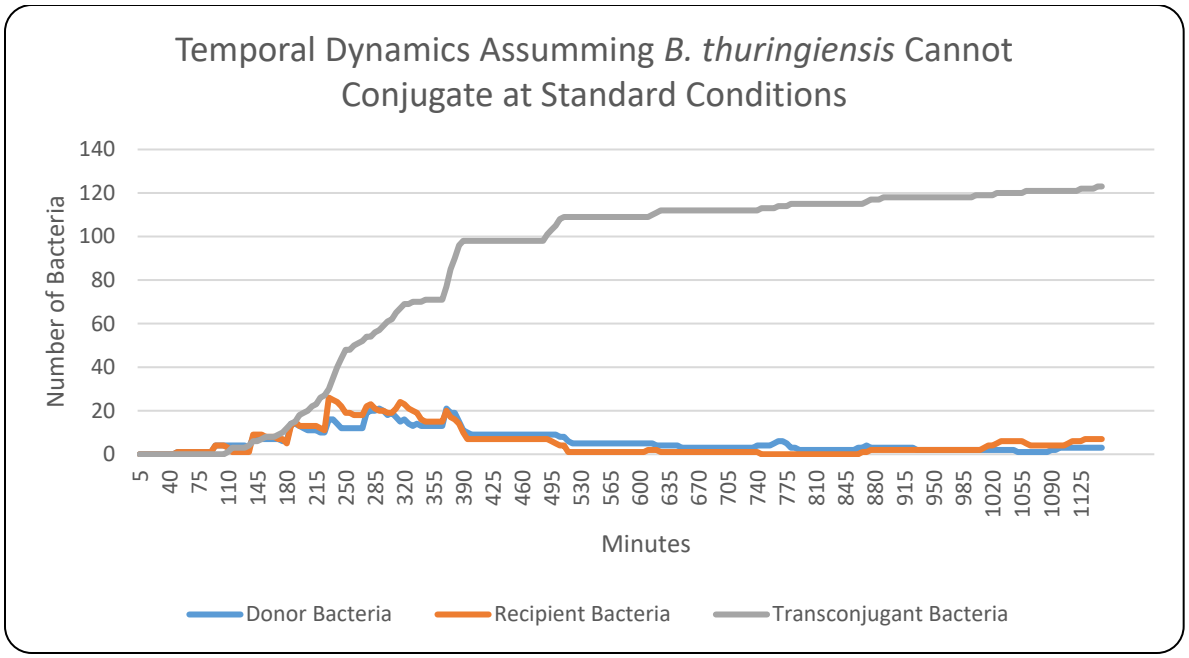

Figure 9. Results of experimental simulation 1 data showing bacterial conjugation temporal dynamics on elongating root surfaces under conditions of 30˚C and 100% relative humidity.

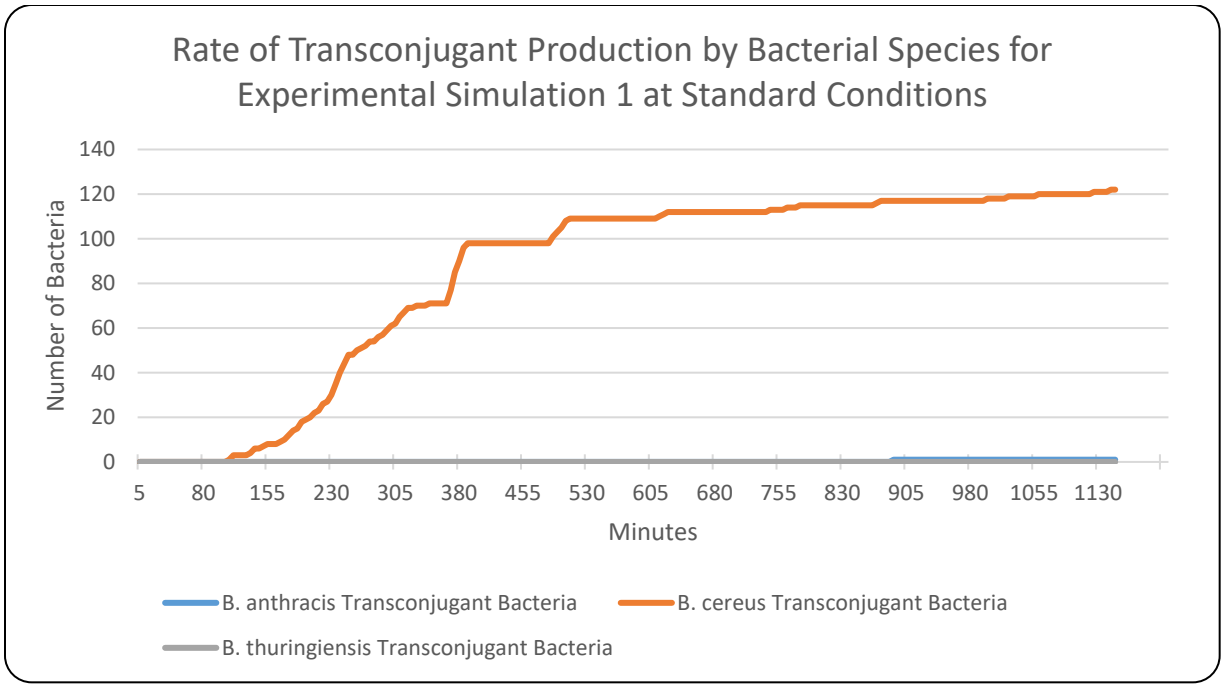

Figure 10. Results of experimental simulation 1 data showing the rate of production of transconjugant bacteria by species, when *B. thuringiensis* cannot conjugate, on elongating root surfaces under conditions of 30˚C and 100% relative humidity.

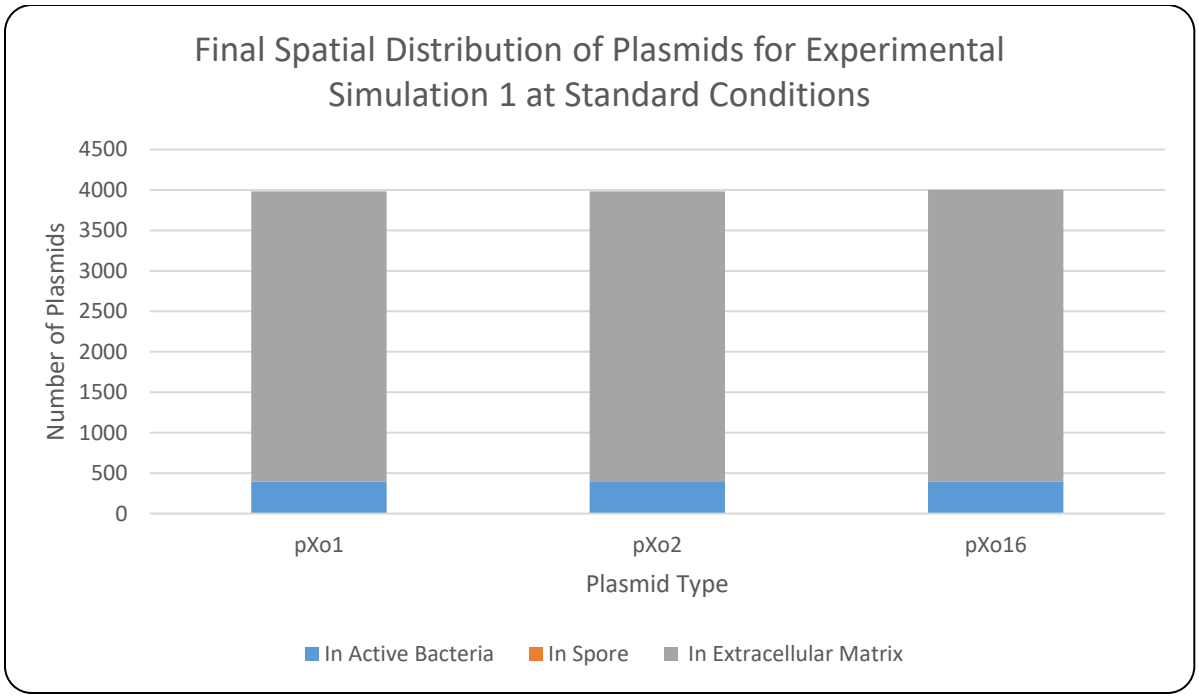

Figure 11. Results of experimental simulation 1 data showing the final spatial distribution of plasmids, when *B. thuringiensis* cannot conjugate, on elongating root surfaces under conditions of 30˚C and 100% relative humidity.